Utrecht University

Master's Thesis – Sustainable Development

Global anthrome exposure to extreme heat in the future

This picture is taken by Jeremy Bezanger and authorized by Unsplash

Student name: Lu Yin (0670496), l.yin1@students.uu.nl

Supervisor: Dr. ir. C.G.M. Kees Klein Goldewijk, c.g.m.kleingoldewijk@uu.nl

Second reader: Dr. Murray Scown, m.w.scown@uu.nl

Date: 2022/07/18 | Master thesis | 45 ECTS

Sustainable Development – Environmental Change and Ecosystems

Faculty of Geosciences – Utrecht University

Summary

Under the context of global warming, the frequency and intensity of extreme heat events will increase in the future, threatening the terrestrial system. This research made efforts to estimate the frequency and influenced area of extreme heat in three future scenarios (ssp126, ssp370 and ssp585) regarding anthrome, human health and 4 major crops(maize, wheat, rice and soybean).

For anthrome, we used the relative threshold (90^{th} percentile) method, and our result suggested that the frequency of extreme heat of all anthrome has a similar increasing trend before 2050 in those three future scenarios. For the next coming periods, the extreme days and areas with more extreme heat remain stable in ssp126 while ssp370 and sssp585 keep increasing in frequency and area with more extreme heat. 2060 is a signal, indicating that all anthromes experience more extreme heat events than the present in ssp370 and ssp585. At the end of the 21^{st} century, The extreme heat days for most anthromes double in ssp126 compared with that of the present, while ssp370 and ssp585 have similar results that extreme heat days increase more than three times

For the human health part, we adopted the wet bulb globe temperature method to quantify population exposure to extreme heat in the future. Extreme heat frequency will mainly occur in tropic and subtropic regions. Population exposed to extreme heat remains stable from 2015 to 2050 for most anthromes in all future scenarios. Then population exposure to heat in ssp126 decreased slightly while it increased quickly in ssp370 and ssp585. For most high population density anthromes, population exposure in ssp126 to heat is close to that of the present at the end of the 21^{st} century. In ssp370 and ssp585, 23%-72% population in different anthromes were exposed to heat.

The daily average temperature was used for the crop part to count extreme heat days. In ssp126, extreme heat days nearly doubled for most crops, while in ssp370 and

ssp585, extreme heat days increased much faster than in ssp126. Especially in ssp585, the extreme heat days increased more than 10 times for most crops, indicating that crops would face poor growing conditions in such an extreme scenario. Among those crops, rice was most influenced by extreme heat, while wheat was least influenced. And there was no significant difference between irrigation and rainfed systems. In general, the more frequent extreme heat in the future will threaten our land system, human health and food security. More attention and mitigation or adaptation strategies are needed to cope with the extreme heat crisis in the future.

Acknowledgement

First, I would like to express my gratitude to my supervisor Kees Klein Goldewijk for his invaluable patience and support, without which I can not finish my thesis smoothly. His patient guidance helped me during this thesis's proposal, research, and writing phase.

Second, I would like to thank two advisors: Murray Scown and Jonathan Doelman, who provided the primary idea and useful insights into this thesis. I also like to thank Jonas Jägermeyr, Christoph Müller, and others who contribute to this thesis. I also want to thank my best friend, Zhouyuan Wang, who gave me feedback and taught me writing skills.

Last but not least, I would like to thank my parents, without none of you this would indeed be possible. We have not seen each other for two years due to COVID-19, and I hope we can reunite soon.

Table of Contents

List of abbreviations

CDO: Climate data operator

CMIP: Coupled Model Intercomparison Project

CMIP6: Coupled Model Intercomparison Project phase 6

ECS: Equilibrium climate sensitivity

GCMs: Global climate models

GGCMI: Global Gridded Crop Model Intercomparison

GHGs: Greenhouse gas

HI: Heat index

HYDE: History database of the Global Environment

IPCC: Intergovernmental Panel on Climate Change

ISIMIP: Inter-Sectoral Impact Model Intercomparison Project

NOAA: National Ocean and Atmospheric Administration

RCPs: Representative Concentration Pathways

SDG: Sustainable development goal

SSP: Shared Socioeconomic Pathways

TCR: transient climate response

WBGT: Wet bulb globe temperature

WGCM: Working Group on Coupled Modelling

List of figures

Appendix:

List of tables

Appendix:

1. Introduction

1.1 Land system

The land system is a sub-system of the earth system, representing the terrestrial component of the earth and including all human activities on land (Verburg et al., 2015). It is the consequence of interactions between human activities and the natural environment (Verburg et al., 2013). The land is of vital importance to the human community because it provides with necessary resources like food, fuel, fibres, other raw materials, and a lot of other ecosystem services as well, which support food production, resist natural disasters, and provides cultural services (Ivanova et al., 2012).

Long before the Holocene period, human ancestors set fire as tools to make hunting easier (Klein Goldewijk et al., 2017), not altering the landscape intensively. In that period, microclimate was regarded as the most crucial factor shaping vegetation patterns and land cover (Mucina, 2019). And the interactions between human societies and the natural environment had been formulated, changing the local evolutionary dynamics, ecosystem, and landscapes (Ellis et al., 2021). Then, humans began to domesticate animals and grow plants. The traditional hunting lifestyle was replaced by permanent settlement and crop supply, transforming the natural landscape into other agricultural land systems such as cropland (Klein Goldewijk et al., 2017; UNCCD, 2017). From then on, humans gradually became the primary driver contributing to the land pattern change. In 4000 CE, the newest land use reconstruction indicated an astonishing result: about 3/4 natural terrestrial ecosystem had already been inhabited and influenced by hunting and agricultural activities (Ellis et al., 2021).

At 1 CE, intensive agricultural and pastoral land use transformation had been underway in Europe, Asia, and other parts of the world. Such intensive land use transformation accelerated after Second World War because the rapidly increasing population and the industrial revolution increased food demand and improved food production. More than 80% terrestrial ecosystem has been altered more or less by human activities, and people's lifestyles have changed completely (Ellis et al., 2021; Sanderson et al., 2018). Most people now live in urban areas, which reshaped the land system irreversibly and adversely. 44% of the land was inhabited by humans and has been influenced more or less by human activities (Jacobson et al., 2019). The future population is projected to increase to about 9.8 billion by 2050 and will increase to 11.8 billion by 2100 (Ogle et al., 2018). Such an increasing population will increase the demand for food, posing more pressure on converting semi-natural land to cropland and pasture area. Most of the highly productive land is being exploited by humans (Lambin & Meyfroidt, 2011), and land scarcity is expected to accelerate because of urbanization and demand for food and resource (Popp et al., 2017).

1.2 Anthrome

Plants form the local biosphere in the land system, although humans have now become the dominator of the Earth (Mucina, 2019). The biotic communities are large spatial scales, and they are named biome together with their environment (Mucina, 2019). In 1916, this new concept was first created by Frederick Clements (Clements, 1916), and then it was widely discussed and redefined by other ecologists for the next 100 years. The concept of biome was well recognized in ecology and biogeography because it can comprehensively indicate the biotic society at a larger geographic scale, which is shaped by climatic factors (Mucina, 2019).

The human race has profoundly influenced the terrestrial system and altered local ecosystem composition by using a lot of natural resources in some areas. It might create a new 'novel ecosystem' that involves human activity and the environment (Morse et al., 2014). Biomes are now still commonly adopted by ecologists as a fundamental tool to classify the patterns of the global ecosystem without any consideration of human influence. However, the biome usually ignores human influence on reshaping land patterns. Recently, a novel and alternative concept, anthropogenic biomes, also named anthrome, was introduced to divide land patterns in terms of land use and population density (Ellis & Ramankutty, 2008). The latest version of the anthrome database has been completed based on the History Database of the Global Environment (HYDE 3.2) and other data input. It used a distribution rule (Fig A-1) of classification and mapped anthropogenic conversion of the terrestrial ecosystem from 12000 BC to 2015 (Ellis et al., 2021). The unpublished future anthrome database from 2015 to 2100 was also finished last year (van der Wielen, 2021), which will be used in this research. The anthrome classification divided land patterns into 20 anthromes, including intensively used land, cultured land and wildland (Ellis et al., 2010). Although various researchers widely adopted this novel land pattern, there is limited research on anthrome in climate change.

1.3 Global warming and extreme heat

The global climate stayed relatively stable about 12800 years ago (Berkman & Young, 2009), providing a suitable environment for human development. Since then, humankind started to populate quickly, reshaping the landscape across the terrestrial biosphere ecosystem and gradually dominating the earth. After 10000 years of stable climate conditions, the air temperature has been increasing quickly since the industrial revolution, and human activities have been the primary driver (Rockström et al., 2009). Since 1750, the world has emitted more than 1.5 trillion tones of CO_2 (Ritchie, 2019), which can absorb longwave radiation and result in a warming planet. In the 21st century, although there is a downward trend in the increase of Green House Gas (GHG) emissions, the total emission has been still increasing stably (IPCC., 2022). Since 1850, the global average temperature has risen about 1°C more than that in the pre-industrial period, which may lead to more pressure on the land system and approach the limited value of 2°C in the Paris Agreement (Rockström et al., 2009; Rogelj et al., 2016). Although different land ecosystems' responses to climate change are not studied thoroughly, extreme climate phenomena associated with global warming can threaten the local human, animals, ecosystem, and society (Luber & McGeehin, 2008). The relationship between increasing air average temperature and extreme weather events has been well explored globally. A small change in average can significantly change extreme heat events and increase the frequency and intensity of extreme heat (Perkins, 2015). In populated areas, observational climate records showed that the frequency and intensity of extreme heat increased significantly, and the frequency of extreme precipitation increased. In contrast, the cold extreme declined, and windy extreme days decreased over the past 40 years (Mishra et al., 2015). As an important part of global extreme events, extreme heat has recently attracted a lot of attention. However, there is no unit or standard to define extreme heat events; various definitions were adopted for different research objectives (Horton et al., 2016).

1.4 Extreme heat hazards

More frequent and intense extreme heat events in the future due to climate change will have negative impacts on human society. Firstly, extreme heat events negatively impact the local economy and threaten human health (Chen et al., 2020). Extreme heat events are also associated with other health hazards such as poor air pollution, wildfires, water scarcity, crop production, and electrical facilities, leading to potential threats to human health (Barriopedro et al., 2011). High-temperature weather can cause a series of physiological changes in the body's temperature regulation system, putting the human body in a condition of ‘overload’, aggravating the disease, and even leading to death. Many deaths worldwide are related to exposure to high temperatures, and the death toll continuously increases due to increasing temperature (Basu & Samet, 2002). In the past 30 years, extreme heat events worldwide have been associated with more than 100000 excess deaths (Horton et al., 2016). However, most past research utilized air temperature as a core metric to assess and estimate the heat stress on human health (Li et al., 2020). However, in a high humid area like South America, air temperature is insufficient to represent extreme heat stress on human health because high humidity air can reduce the efficiency of sweat evaporation, leading to a much hotter body 'feel' temperature. In 1950, a new heat stress indicator for human health, wet bulb globe temperature (WBGT), was developed to assess heat-related disease and is now widely accepted (Grahame M Budd, 2008). It contains not only air temperature, but also involves other climate variables such as relative humidity, cloud cover, and sun angle to provide a better understanding of heat stress (National Weather Service, 2022).

Extreme heat can influence crop growth and production as well. Although different crops respond differently to global climate change, increasing the frequency and intensity of extreme heat events related to climate change can reduce crop productivity. Food security is regarded as one of the most important goals to meet the food demand of the increasing population (Kang et al., 2009). In agricultural areas, extreme events associated with climate change may influence local agriculture activity and food system infrastructure, which might also threaten global food security. When the air temperature exceeds a certain threshold, extreme heat can increase leaf senescence and influence crop yield. Crop models are usually used to explore the crop production response to future climate change. However, only part of global crop models considers the impact of extreme heat. Maize, soybean, wheat and rice contributed 90% of the worldwide caloric production of all cereals and soybean (Jägermeyr et al., 2021). A global analysis revealed that the latest global gridded crop models underestimate the effects of extreme heat and drought on those four crops (Heinicke et al., 2022), indicating that more frequent and intensive extreme heat events might pose more severe threats to food security. Therefore, it is necessary to give a more detailed investigation to explore the future extreme heat with consideration of specific crops.

1.5 Future scenarios

Because of the uncertainty of the future, the scenario approach is widely adopted and plays an essential role in climate change research (Riahi et al., 2017). It can provide plausible socio-economic and climate pathways for the future, including changes in various socioeconomic and climate variables such as land use and cover, technology, economic growth and emission of greenhouse gas (van Vuuren et al., 2011). Those scenarios are essential elements for climate change models and the basis of climate change assessment for government and policymakers (van Vuuren et al., 2011).

The concept of Representative Concentration Pathways (RCPs) was introduced recently and provided plausible climate pathways for model communities to conduct long-term climate experiments (Moss et al., 2010). RCPs indicated the future greenhouse gas emission that led to future radiative forcing relative to pre-industrial. However, socioeconomic descriptions of the future to fit RCPs were still missing. Therefore, a novel design and structure of a plausible socioeconomic lot, Shared Socioeconomic Pathways(SSP), was proposed to match different climate scenarios with quantitative and qualitative descriptions of elements (van Vuuren et al., 2014). There are five SSPs: SSP1 represents the sustainable future with low challenges to mitigation and adaptation; SSP2 refers to the middle of the road with medium challenges to mitigation and adaptation; SSP3 indicates regional rivalry with high challenges to mitigation and adaptation; SSP4 describes inequality road with low challenges to mitigation, high challenges to adaptation; SSP5 showed high fossil fuel development with high challenges to mitigation, low challenges to adaptation (Riahi et al., 2017). These different SSP storylines were combined with RCPs to develop a comprehensive climate and socioeconomic future story. The matrix method is used to produce different SSP-RCP scenarios to explore plausible futures and compare with different future scenarios.

1.6 Problem definition

The earth is warmer in all future scenarios, leading to more frequent and intense extreme heat events. As discussed above, extreme heat can negatively impact the land system, such as human health and crop production. Various studies tried to explore and quantify the extreme heat events under different future plausible scenarios.

The relationship between global warming and extreme heat events has been explained well. A small change in average air temperature can significantly change the frequency and intensity of extreme heat (Fischer & Knutti, 2015). However, research on extreme heat events in large-scale land patterns is still limited. The macroclimate was regarded as the most important factor that shaped the large-scale regional biome (Mucina, 2019). From 8000 years ago, human has been reshaping landscape patterns due to intensive agricultural activities and urbanization. In the future, human activities will still be the dominant factor contributing to land use and cover change. The new land use and cover concept, anthrome, provides a novel framework to classify land patterns on land use(cover) and vegetation type and takes population density as a classification criterion. It might be more suitable to use anthrome for current global and large-scale research than the traditional and widely used concept, biome, which ignores that humans have impacted more than 80% of land worldwide. Although anthromes are well recognized by introduction, no research explores the extreme heat events based on large-scale land use and cover system.

For human health, research comprehensively quantifies extreme heat events and their impact (Tuholske et al., 2021). The most studies focused on the past without projection of the future. Besides, past research focused on the urban areas and adopted daily air average or maximum temperature as a threshold to identify the extreme heat, other factors such as air humidity were ignored. Therefore, quantification of extreme heat in the future by adopting the WBGT method and new land classification is necessary.

The food system is vital to human society and will be threatened by more frequent and intensive extreme heat in the future. However, different crops' tolerance to heat extremes is different from each other, and the planting period of crops is inconsistent globally and regionally, making it difficult to conduct a detailed quantification of the whole agricultural land. Besides, most crop models ignore the extreme heat's direct impacts on crop productivity. Therefore, global and precise quantification of extreme heat on specific crops under plausible future scenarios is also needed.

1.7 Research objective

As mentioned above, there is no research exploring the extreme heat events in the future in terms of anthrome perspective. This research aims to quantify the frequency of extreme heat events with a focus on anthromes, human health, and major crops under different future scenarios by giving different extreme heat definitions. The combination of future anthrome and projections of climate models can be implemented to explore the trend of future extreme heat in different regions of the world.

The main research question is: How will extreme heat events change over time globally under different future climate and socio-economic scenarios?

The following sub-questions will answer the main research question:

- How will the extreme heat events change over time in the future for different anthromes?
- How many people will be exposed to extreme heat events at the end of the 21st century under different scenarios?
- What will the frequency of extreme heat change in major crop-growing areas over time?

1.8 Scientific and social relevance

In the context of global warming, the frequency and intensity of extreme heat events will increase in the future (Allan et al., 2021), threatening the terrestrial system, human health, and food security. Anthrome, a new land classification method, re-defines the biome by considering the interaction between humans and the ecosystem (Ellis & Ramankutty, 2008). The past study examined the extreme heat events in the global aggregate or focused on a small region, seldom considering the specific land patterns(biome) as a whole. There is limited scientific research quantifying extreme heat events from in anthrome perspective. Such investigation is especially needed, providing current research with climate information that is useful for biome risk assessment and decision-making. Besides, past studies that investigated heat stress for humans always used air temperature as the only indicator, ignoring humidity and other climate variables (G. M. Budd, 2008). Evidence proved that humidity has a close relationship with breath, and high relative humidity can influence perspiration. Unlike human health, which has attracted a lot of attention, the direct impacts of extreme heat on crops have been neglected. High air temperature can accelerate the phenological development and reduce the growing season length (Jägermeyr et al., 2021). However, most crop models cannot simulate the direct impacts of extreme short-term heat on crops (Jägermeyr et al., 2021).

This research made efforts to explore extreme heat events with considering human health and crops by adopting more accurate extreme heat definitions. Studies conducted thorough research on extreme heat events in the past without considering the future. Therefore, this research combines the Anthrome and scenarios perspectives to create a plausible future extreme mapping, contributing to the growing literature on extreme heat events. Investigating the future extreme heat events is a critical advance to understanding how extreme heat influence the terrestrial system, human, and food security.

Besides scientific contribution and relevance, quantifying extreme heat by using the Anthrome land patterns for future scenarios is also very important for decision-makers to develop relevant climate adaptation and mitigation policies and strategies. In 2015, 17 Sustainable Development Goals(SDGs) were introduced in The 2030 Agenda for Sustainable Development to build a peaceful and prosperous world (Sachs et al., 2021). However, many of them will be influenced by more frequent and intense extreme events (SDG 2, 3, 8, 11, 13, 15). Extreme heat events usually directly influence mortality and hospitalizations (Horton et al., 2016). Heat stress also affects specific regions and racial groups and causes societal and economic consequences (Council, 2021), increasing inequality between regions and races. With the growing population, the demand for food is also increasing. The rising food demand and more frequent and destructive extreme heat in the future will increase the risk of food security. Therefore, a comprehensive assessment and quantification of extreme heat events in terms of human health and food safety are necessary to provide policymakers, local government and investors, especially those in tropic and subtropic areas, with quantitative and convincing evidence on the agriculture and human society and terrestrial system dimensions of the challenge.

2. Method

2.1 Research framework

This research is divided into parts: (1) extreme heat days for anthrome, (2) heat stress for humans, (3) extreme heat for crops. These three parts are explored separately using different extreme heat definitions per year in future scenarios. The frequency(days) of extreme heat events is chosen as the core indicator in this research. Hence, the first step is to give extreme heat definitions and find suitable heat thresholds. Days that daily temperature is higher than this threshold can be counted and utilized as the frequency of extreme heat. A combination of relative heat threshold and absolute thresholds methods is applied to this research with consideration of different research parts:

1. Wet bulb globe temperature((Eyring et al., 2016)WBGT) for humans (Iso, 2017; Tuholske et al., 2021)
2. Relative daily maximum(90^{th}) temperature for anthrome land system (Chen et al., 2020; Sulikowska & Wypych, 2020)
3. Literature review of air temperature threshold for different crops (Wahid et al., 2007)

After the definitions of extreme heat thresholds, the future climate parameters will be collected to estimate the extreme heat days. The future climate variables are derived from Coupled Model Intercomparison Project phase 6 (CMIP6) (Eyring et al., 2016). Five bias-adjusted subsets GCMs of CMIP6 have been selected: (1) GFDL-ESM4, (2) IPSL-CM6A-LR, (3) MPI-ESM1-2-HR, (4) MRI-ESM2-0, and (5) UKESM1-0-LL (Lange, 2021). The SSPs can be integrated with RCPs to create new future scenarios, and three future scenarios are selected to conduct this research that is SSP1-RCP26, SSP3-RCP70, and SSP5-RCP85 (hereafter 'ssp126', 'ssp370' and 'ssp585') (Riahi et al., 2017). Then, to estimate different extreme indicators, three corresponding climate variables are extracted from five GCMs for three future scenarios: (1) Near-surface daily air temperature, (2) Near-surface daily maximum temperature, and (3) Near-surface relative humidity (Lange, 2021). Different climate variables can be adopted in different research parts (see arrows in Fig 1). Finally, extreme heat days for each GCM and future scenarios are calculated for each research part individually.

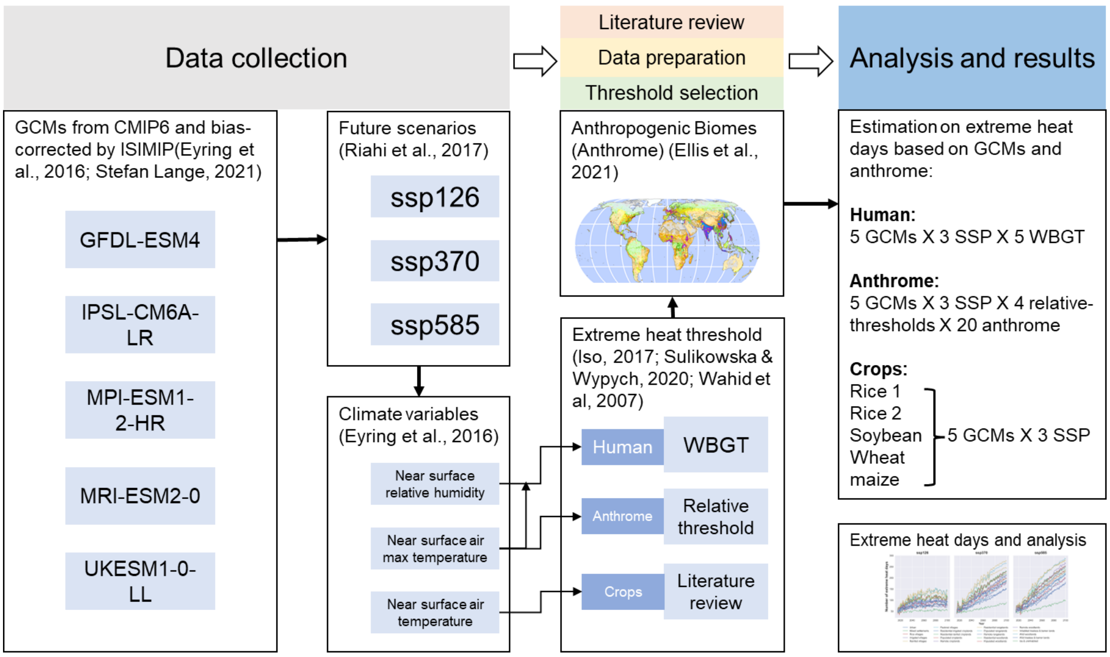

Figure 1: research framework. The framework shows the research process and helps answer research questions. It includes five parts and starts from the left: (1) data collection (2) literature review (3) data preparation (4) threshold selection (5) analysis and results. The data collection part mainly shows what selected GCMs, future scenarios, and climate variables. The literature review focuses on how extreme

heat threshold on human health, crop growth, and land system (anthrome). Data preparation also includes some database input such as land use, crop calendar, and population database, and that inconsistent dataset will be harmonized. The analysis and results show how different research parts will be conducted.

2.2 Climate forcing database input

This research focuses on quantifying extreme heat events under different future scenarios. Core modelling outputs such as climate variables, land-use change and cover, crop calendar, and crop area are derived from different institutes and are harmonized across various research sectors. Subset climate databases are selected from the CMIP6 project to analyze extreme heat days. CMIP is a project under the Working Group on Coupled Modelling (WGCM) sponsorship, providing a framework to improve climate change knowledge (Eyring et al., 2016). The project began in 1995 and now involves more than 30 climate models and is widely used in numerous scientific research. These models can give a better understanding of past, present, and future global climate change (Eyring et al., 2016). However, more and more different GCMs have participated in CMIP6, leading to more considerable uncertainty of future climate change. Some GCMs are ‘too hot’: overestimating global warming (Hausfather et al., 2022). Thus, choosing suitable GCMs is essential. Two main indicators can be used as a standard to select GCMs with good performance: (1) transient climate response (TCR); (2) equilibrium climate sensitivity (ECS). TCR is the total amount of warming in the year when atmospheric CO2 concentrations double after a fixed increase of 1% every year. The second similar metric, ECS, is defined as the final long-term temperature response to CO2 concentrations that doubled. These two indicators are similar but distinct, but models with higher TCR usually tend to get higher ECS (Hausfather et al., 2022). A consensus was developed by IPCC working groups that research is encouraged to adopt climate models with better behaviour, which can make research results more consistent and comparable with the AR6 report (Hausfather et al., 2022). Besides adopting TCR and ESC, the selection of databases is also based on daily data availability, historical behaviour, and structural independence (Lange, 2021). However, the raw databases of GCMs are always low resolution because of potential expensive computational costs (Enayati et al., 2020). Thus, statistical downscale techniques are adopted by scholars to process and re-calibrate the raw dataset.

Table 1: description of global climate models(GCMs)

GCM	Member	Bias-corrected method	ECS(°C)	TCR(°C)
GFDL-ESM4	r1i1p1f1		2.63	1.63
IPSL-CM6A-LR	r1i1p1f1		5.18	2.35
MPI-ESM1-2-HR	r1i1p1f1	ISIMIP3BASD	3.34	1.64
MRI-ESM2-0	r1i1p1f1		3.42	1.67
UKESM1-0-LL	r1i1p1f2		5.49	2.77

The Inter-Sectoral Impact Model Intercomparison Project (ISIMIP) is a framework that consistently assesses the impacts of climate change on different sectors (Warszawski et al., 2014). ISIMIP selected five climate databases, three of which had relatively lower ECS and TCR: (1) GFDL-ESM4 (2) MPI-ESM1-2-HR (3) MRI-ESM2-0, and the other two databases have relatively higher TCR and ECS: (4) IPSL-CM6A-LR (5) UKESM1-0-LL. The benefit of using an ensemble of a subset of the CMIP6 project is to reduce projection uncertainty. The raw databases of five GCMs (Table 1) have biases and different resolutions. Therefore, they are downscaled to 0.5°X0.5° at daily time steps and bias-corrected by ISIMIP (Lange, 2021). ISIMIP used a new bias-corrected method and statistical downscale strategy to reproduce better performance and fine resolution datasets (Lange, 2019). This research adopted these five climate forcing models' output. To lower the uncertainty of future projections, all the analyses based on climate databased will be conducted separately instead of taking the mean values.

2.3 Scenarios selection

This study adopted a matrix approach to combine different SSPs and RCPs. There were four key combined scenarios: (1) SSP5-RCP8.5, (2) SSP3-RCP7.0 (3) SSP2-RCP4.5 (4) SSP1-RCP2.6. And other additional scenarios were also provided, and the detailed description of these key and supplement scenarios were well explained in O'Neil's paper (O'Neill et al., 2016). Due to the dataset availability and time limitation, this research, of course, focused on three key (Tier 1) future scenarios: ssp126, ssp370, and ssp585, which were used to quantify extreme heat events with consideration of terrestrial system (anthrome), human health and four major crops. The detailed information about different parts in terms of various SSP-RCPs is illustrated in Table 2.

Table 2: key elements among selected scenarios related to climate and land use(cover) change. This table is retrieved and modified from (Popp et al., 2017)

SSP-RCP element	**ssp126**	**ssp370**	**ssp585**
General pathway	Sustainability	Regional rivalry	Fossil-fueled development
Climate forcing (O'Neill et al., 2016; van Vuuren et al., 2011)			
Radiative forcing change	Sustainable forcing pathway(2.6 W/m^2)	Stabilization of forcing pathway(7.0 W/m^2)	Increasing radiative forcing pathway(8.5 W/m^2)
Population growth (Jones & O'Neill, 2016)			
High fertility	Low	High	Low
Other low fertility	Low	High	Low
Rich low fertility	Medium	Low	High
Total(2050/2100,billion)	8.5/7.0	10.0/12.8	8.6/7.4
Land-use change (Popp et al., 2017)			
Land-use change regulation	Strong regulation	Limited regulation	Medium regulation
Land productivity growth	High improvements in crop production	Low improvement	High-intensive resource management, high improvement
The environmental influence of food consumption	Low meat-based diet, low food demand	Resource intensive consumption	High meat-based diet, intensive food consumption
Land-based mitigation policies	Good cooperation for climate change mitigation	Heavily delayed cooperation for climate change mitigation, limited participation	Delayed cooperation, full participation

Ssp126 illustrates the sustainable pathway of the earth's future scenarios with more respect to environmental protection. The goal of ssp126 is to limit the increasing temperature to 2°C at the end of this century. The whole world will change slowly towards the ideal path. The emission of greenhouse gas will be well limited, leading to a peak radiative forcing level of 3.0 W/m^2 and then will decrease to 2.6 W/m^2 at the end of this century. Land use is strongly regulated, and crop production is significantly improved due to the development of agricultural technology worldwide (Popp et al., 2017). The population will increase to 8.5 billion and then decrease to 7.0 billion in 2100, not putting too much pressure on the terrestrial system. Ssp370 implies a rocky way. More conflicts will occur between regions, and countries focusing more on domestic development and growing nationalism will prevent globalization (Popp et al., 2017). The emission of GHGs will continue to increase until the radiative forcing level reaches 7.0 W/m^2. The population will grow rapidly to 12.8 billion at the end of this century. There will be limited land use limitations and no apparent improvement in agricultural technology because of low international cooperation. Ssp585 describes a highway based on fossil fuel development. There will be increased confidence in the competitive market due to the successful industrialization and emerging economics, contributing to a more globalization world. The GHGs will be emitted unlimitedly, and the radiative forcing level will arrive at the highest level: 8.5 W/m^2. Like ssp126, ssp585 sees a rapid development, and of course, more investment will be implemented in education and health, causing a relatively slow population growth (Jones & O'Neill, 2016), which will increase to 8.6 billion in 2050 and decline to 7.4 billion in 2100. The regulation of land use will not be well limited, and highly intensive management of agricultural land and improved agricultural technology will develop.

2.4 Extreme heat threshold protocol

The research objects of this study are anthrome, human, and four major crops. Each of them has a different response and tolerance to extreme heat events. Therefore, various definitions of extreme heat thresholds should be developed for each element.

Wet bulb globe temperature (WBGT)

For human health, wet bulb globe temperature (WBGT) is adopted in this research. WBGT consists of three variables: (1) dry air temperature(T_a), (2) natural wet bulb temperature(T_{nw}), and (3) globe temperature(T_g) (Liljegren et al., 2008). And the linear relationship between WBGT and these three climate variables is shown in the formula below:

$$WBGT = 0.7T_{nw} + 0.2T_g + 0.1T_a \tag{1}$$

WBGT was created in mid 20th century and was firstly used in the US army as an important indicator to control heat-related illnesses (Grahame M Budd, 2008). Although it has some limitations, such as measurement errors and restricted evaporation of sweat, WBGT has been widely adopted as heat stress guidelines for outdoor work and sports combined with the international standard ISO 7423 (Iso, 2017). As is shown in Table 2, different metabolic rate work corresponds to different WBGT thresholds. Here metabolic rates represent different labour intensity; metabolic rate < 65 Wm^{-2} refers to resting at easing; metabolic rate between 65 Wm^{-2} and 130 Wm^{-2} refers to light manual work such as writing and typing; metabolic rate between 130 Wm^{-2} and 200 Wm^{-2} refers to sustained arm, leg or trunk work such as weeding and hoeing; metabolic rate between 200 Wm^{-2} and 260 Wm^{-2} refers to some intense arm or trunk work such as carrying heavy materials; metabolic rate above 260 Wm^{-2} refers to very intense activities such as working with an axe or climbing stairs (Iso, 2017). Furthermore, there are two WBGT reference levels: acclimatized and not acclimatized. Acclimatization to heat is usually a beneficial physiological adaptation that happens when persons repeatedly work or live in a hot environment (CDC, 2018). And there is a higher WBGT threshold for persons who are acclimatized to heat compared with persons who are not acclimatized to the heat. Therefore, in this research, 30°C is selected as the threshold (Tuholske et al., 2021) and other acclimatized WBGT thresholds (25°C, 26°C, 28°C and 33°C) are also analyzed to explore threshold sensitivity.

Table 3: WBGT reference level (ISO 7423)

Metabolic rate(Wm^{-2})	WBGT reference level	
	Acclimatized(°C)	Not acclimatized(°C)
<65	33	32
65-130	30	29
130-200	28	26
200-260	26	23
>260	25	20

However, the measurement of WBGT usually has a strict requirement, and separate sensors are needed to measure the three climate parameters above (Formula 1). Therefore, it usually can not be calculated directly by using meteorological data. Adopting empirical formulas or models is widely used in recent research with satisfactory results (Li et al., 2020; Liljegren et al., 2008; Tuholske et al., 2021). Therefore, I use near-surface daily maximum temperature(T_{max}) and near-surface daily relative humidity(RH) to simply estimate the daily WBGT from 2015 to 2100 under different SSPs and GCMs. The first step is to calculate the daily heat index(HI) by adopting the National Ocean and Atmospheric Administration's(NOAA) method (NOAA, 2014). The empirical analysis of regression was conducted by Lans P. Rothfusz and the formula is shown below:

$$HI = -42.379 + 2.04901523 * T + 10.14333127 * RH - 0.22475541 * T * RH - 0.00683783 * T * T - 0.05481717 * RH * RH + 0.00122874 * T * T * RH + 0.00085282 * T * RH * RH - 0.00000199 * T * T * RH * RH \tag{2}$$

T is the daily maximum temperature in degrees F and RH refers to the daily relative humidity in percentage(%). While, in some conditions, the performance of the formula is not accurate and needs adjustment. When relative humidity is less than 13% and temperature is between 80 and 112 degrees, the adjustment should be subtracted from the HI formula:

$$AD = [(13 - RH)/4] * sqrt\{[17 - abs(T - 95)]/17\}$$

(3)

Where abs refer to absolute value, AD means adjustment and sqrt is the arithmetic square root. When the relative humidity is greater than 85% and air temperature ranges from 80 to 87 degrees F, the adjustment below will be added to the HI formula:

$$AD = [(RH - 85)/10] * [(87 - T)/5]$$

(4)

However, the HI formula is not suitable when the temperature is lower than 80 degrees F. the following new HI formula is implemented:

$$HI = 0.5 * \{T + 61 + [(T - 68) * 1.2] + (RH * 0.094)\}$$

(5)

The algorithm above is adopted to calculate the daily heat index, and then an empirical second-order power relationship can be used to transfer HI to WBGT for each grid (Bernard & Iheanacho, 2015). The formula is shown below:

$$WBGT = -0.0034HI^2 + 0.96HI - 34$$

(6)

Where WBGT is in degrees Celsius(°C), HI is in degrees F. The final daily WBGT product will be done following all steps mentioned above.

Extreme heat threshold for land system (anthrome)

Another part of this research is to quantify the extreme heat events for large-scale land patterns: anthromes. However, a unit and standard extreme heat threshold for a large-scale land system are hard to develop because different biomes and different locations can lead to unequal responses and tolerances to extreme heat events. Therefore, a relative threshold approach will be adopted in this part. The extreme heat threshold for anthrome is defined as the 90th percentile of daily maximum air temperature for the base period (Sulikowska & Wypych, 2020). I will calculate the extreme heat days of every year from 2015 to 2100 under different future scenarios. Other percentile thresholds (80th, 95th, 99th) are also chosen to explore the sensitivity to different temperature thresholds. One objective of this research is to compare future extreme heat frequency with the present. Therefore, a base period for the present from 1985 to 2014 is selected to develop an extreme heat threshold. W5E5 v2.0 is an observational climate database providing the globe's record climate variables at 0.5°X0.5° and daily spatial resolution from 1979 to 2019 (Lange et al., 2021). It is widely used to support bias adjustment for climate model simulations. The 90th (80th, 95th, 99th) percentile air maximum temperature is extracted from W5E5 v2.0 from 1985 to 2014 at each grid as the threshold to quantify extreme heat events.

Temperature threshold for crops

For crop parts, I focus on four major crops, maize, wheat, soybean, and rice. These four main crops contribute 90% of today's global cereal and soybean production (Jägermeyr et al., 2021). The first step is to conduct a comprehensive literature review on heat stress on these crops. However, thresholds between different kinds of literature are not consistent. Besides, different stages of crop growth usually have different heat tolerance (Kilasi et al., 2018; Poudel et al., 2020; Tiwari & Yadav, 2019). Therefore, to determine threshold units and consistency, this research adopts a simple rule when looking for the temperature threshold of crops, that is, the daily mean temperature where a detectable reduction can be observed in crop growth.

Table 4: daily mean temperature threshold of four major crops

Crop type	Temperature threshold(°C)	Reference
Maize	35	(Sabagh et al., 2020a)
Soybean	35	(Sabagh et al., 2020b)
Rice	32	(Kilasi et al., 2018)
wheat	35	(Poudel et al., 2020)

As Table 3 shows, different thresholds for four crops are selected. Maize usually can bear moderate high air temperature, but long exposure to temperatures above 35°C is unfavourable and can lead to yield loss (Sabagh et al., 2020a). For rice, different growth stages have different favourable air temperatures. Therefore, 32°C is selected because temperatures above 32°C can negatively influence all stages of rice growth and development (Kilasi et al., 2018). For soybean, the yield can be reduced significantly when exposed to a temperature above 35°C for more than 10 hours (Sabagh et al., 2020b). For wheat, although different growth has different suitable temperatures, exposure to a temperature above 35°C for a short time can contribute to a significant loss in yield (Poudel et al., 2020).

Crop calendar and assumption

To estimate extreme heat days for crops, some strategies and assumptions are adopted in this research. Global Gridded Crop Model Intercomparison (GGCMI-CMIP6) is a project that simulates crop production under different future scenarios by employing various grid crop models and additional products (Jägermeyr et al., 2021). The growing seasons of various crops are different for different crops and regions. Therefore, the GGCMI crop calendar is implemented to help exclude the days when there is no crop growing (Jonas Jägermeyr, 2021). The GGCMI crop calendar integrated different observational datasets and provided the planting date and maturity date of 18 different crops by a basic rule with more respect to the regional product (Jonas Jägermeyr, 2021). All the data were rasterized to a 0.5° x 0.5° grid to match crop models.

Table 5: data source of GGCMI crop calendar product

Name	Resolution	Source
	Global crop calendar product	
SAGE	5’ x 5’	(Sacks et al., 2010)
MIRCA2000	5’ x 5’	(Portmann et al., 2010)
GSHW	0.5° x 0.5°	(Iizumi et al., 2019)

RiceAtlas	$1km^2$ grid	(Laborte et al., 2017)
ECJRC	0.5° x 0.5°	(Whitcraft et al., 2015)
National dataset		
Brazil: CONAB		(CONAB, 2019)
China: ChinaCropPhen1km		(Luo et al., 2020)
India: Ministry of Agriculture Agricultural Statistics at a Glance 2018		(India, 2018)
Australia: ABARES		(Australian Bureau of Agricultural and Resource Economics and Sciences, 2010)

I assume that the historical and current GGCMI crop calendar is also applied to different future scenarios, making it consistent with the GGCMI project hypothesis. To keep the assumptions consistent with the GGCMI-CMIP6 project, I follow GGCMI's bold assumption that fixed land use of different crops in 2015 is used in this research. The irrigation and rainfed areas are distinguished among these four major crops and analyzed separately. For rice, two rice growing seasons (rice1 and rice2) are offered in the crop calendar and will be analyzed individually as well. The uncertainty and limitation of the two main assumptions will be in the discussion part.

2.5 Frequency calculation

The frequency of extreme heat events can describe the hazard of extreme heat events (Chen et al., 2020). The first part is to quantify the extreme heat events in terms of the anthrome. As has been discussed above, it is hard to specify an extreme heat threshold for different anthrome. Therefore, a relative threshold method is implemented in this part. The 90^{th} percentile of daily maximum air temperature from 1985 to 2014 is extracted as the reference threshold. For each grid, the extreme heat event takes place if the daily air maximum temperature is bigger than the reference threshold. The formula below is shown:

$$N = \sum_{i=1}^{365(366)} (AMT_i > RTE)$$

(7)

Where N is the extreme heat days for every grid in one year, AMT_i refers to air maximum temperature at date i in one year, and RTE is the reference threshold in every grid. At last, a product containing the frequency of extreme heat from 2015 to 2100 for each grid can be completed. Then, the average frequency of each anthrome is calculated as the indicator to represent the results. Because each grid area of the World Geodetic System varies with longitude and latitude, the formula below is used to calculate the mean frequency of each anthrome:

$$Mean\_fre_x = \frac{\sum_i^{tol} frequency_i * area_i}{\sum_i^{tol} area_i} \tag{8}$$

Where $mean\_fre_x$ is the mean frequency of the corresponding $anthrome_x$, tol is the total amount of gird of each $anthrome_x$, and $area_i$ refers to the area of each grid.

A similar method is implemented based on their corresponding climate variables (WBGT for humans, air temperature for crops) and relevant regions for human health and crop thresholds. The 6 high-density anthromes are chosen for the human part to quantify how much the population will be exposed to extreme heat. The area exposed to heat for crops will be estimated to represent the results. All the calculations and analysis will be processed in Python(3.97) and CDO(1.9.10) on Linux online server.

2.6 Data collection and harmonization

All the datasets needed in this research are listed in Table 6. Among them, three climate variables are sourced from ISIMIP (Stefan Lange, 2021). Historical daily maximum air temperature (W5E5 v2.0) is also extracted from ISIMIP (Lange et al., 2021). Population density (Bryan Jones et al., 2015) and future anthrome (van der Wielen, 2021) are also acquired. Crop calendar (Jägermeyr et al., 2021) and cropland use provided additional information in this research.

Table 6: database input summary for this research

Name	Data type	Resolution	Period	Source
		Climate databases		
GFDL-ESM4	Tmax, RH, T	0.5° x 0.5°	2015-2100	ISIMIP
IPSL-CM6A-LR	Tmax, RH, T	0.5° x 0.5°	2015-2100	ISIMIP
MPI-ESM1-2-HR	Tmax, RH, T	0.5° x 0.5°	2015-2100	ISIMIP
MRI-ESM2-0	Tmax, RH, T	0.5° x 0.5°	2015-2100	ISIMIP
UKESM1-0-LL	Tmax, RH, T	0.5° x 0.5°	2015-2100	ISIMIP
W5E5 v2.0	Tmax	0.5° x 0.5°	1929-2014	ISIMIP
		Socioeconomic database		
Population	Population density	2.5' x 2.5'	2006-2100	(Jones et al., 2015)
Anthrome	Land use	5' x 5'	2010-2099	(van der Wielen, 2021)
		Agriculture database		
Crop calendar	4 major crops	0.5° x 0.5°	Current	(Jägermeyr et al., 2021)
Crop land use	4 major crops	0.5° x 0.5°	2015-2100(2015)	ISIMIP

After data collection, all climate forcing databases have separate 10 years time step files and need to be integrated over time. CDO is used with a merge-time function to process all individual files into a single file from 2015 to 2100. In the data process phases, the resolution of different products is not consistent with each other. Therefore, dataset harmonization is required to produce a consistent resolution for different research phases. The frequency product (0.5°X0.5°) for anthrome and human parts are interpolated and remapped to 5'X5' resolution files to match the anthrome land-use dataset through the nearest neighbour algorithm in CDO. The nearest neighbour remap method uses values nearest to the new grid location, preserving the original values (Baboo & Devi, 2010). The old frequency pixel (0.5°X0.5°) is remapped to 36 new pixels(5'X5'), and all values of the new pixels have the same values as the old pixel. The population density databases are converted into population per grid files by multiplying each grid area. Then, the 2.5'X2.5' population product is resampled to 5'X5' files by using the *gridboxsum* function in CDO. This remap method sums up the values of 4 pixels to create a new pixel, suitable for remapping the population dataset.

2.7 Data analysis and visualization

As summarized in Table 6, several climate forcing and socioeconomic databases are collected and harmonized in this research. Then all files and databases are processed through Python (3.9.7) to create frequency files from 2015 to 2100 for three research phases individually. To present the results, several analysis methods and visualization skills are needed.

For the anthrome part, to assess the frequency of spatial change in the future globally, the frequency of extreme heat events will be mapped globally for different future scenarios and compared with that of the base period. To quantify the frequency of extreme heat and land area affected by heat from 2015 to 2100 for each anthrome, global frequency datasets are overlayed on the anthrome database to calculate the mean frequency separately (equation 8). For the human part, to show spatial frequency change based on WBGT thresholds, the frequency of extreme heat will be mapped globally for different scenarios as anthrome parts do. To quantify how much population is exposed to extreme heat events from 2015 to 2100, the WBGT frequency databases will be overlayed on six high-density population areas: (1) urban (2) mixed settlements (3) rice villages (4) rainfed villages (5) irrigated villages (6) pastoral villages to estimate population exposure to heat events. A similar operation will be conducted in the crop part, but the crop analysis adopts fixed land use instead of the dynamic land pattern (anthrome).

3. Results

The results are divided into three parts to present the quantification of anthrome, population, and crops separately. The first part presents the results of future extreme heat events for 20 anthromes and the total area influenced by more extreme heat events. The second part indicates the frequency of extreme heat for human health and population exposure to extreme heat over time, indicating the hazards of heat stress for humans. In the third part, each crop's frequency of extreme heat and planting area influenced by extreme heat illustrates the trend and potential hazards to future crop planting.

3.1 Anthrome

Frequency of extreme heat days

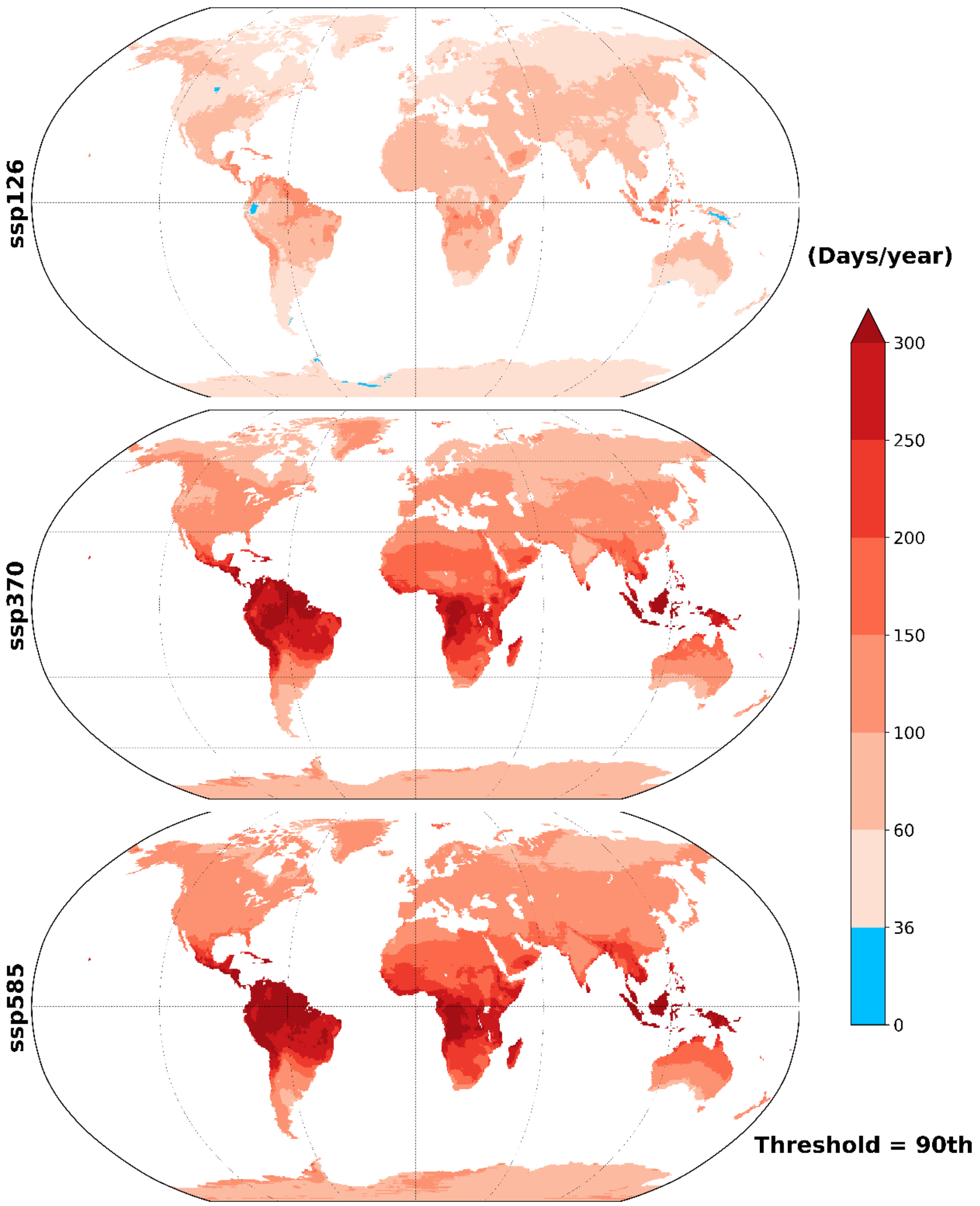

Figure 2: frequency of extreme heat of terrestrial system at 2100, mean values of frequency in five GCMs. Bule parts represent that area experiences less extreme heat than the base period(1985-2014, 36.5 days per year). Red parts show the area that experiences more extreme heat than the base period (means extreme heat days < 36.5 days per year).

As is shown in Fig 2, the frequency of extreme heat events increased for all future scenarios (ssp126, ssp370, ssp585). But the increasing trends and degrees varied among different scenarios. Firstly, the extreme heat days of ssp126 increased more than that of the base period in most regions (base period: 1985-2014, 90th percentile, referring to 36.5 days per year). In some regions, such as South America and Southeast Asia, the frequency decreased compared to the base period (see blue parts in Fig 2, ssp126). High frequent extreme heat days were observed in tropical areas but were limited to less than 100 days at the end of the 21st century.

Results were totally different for the other two scenarios, ssp370 and ssp585 (Fig 2). All regions of the world experienced more extreme heat days than the present. Ssp370 and ssp585 had more extreme heat days compared with ssp126. Extreme heat days in ssp370 and ssp585 were longer than 150 days in most regions of the world. South America, north of Africa, Southeast Asia, and other tropical or subtropical areas had a faster ascent in the frequency of extreme heat than other regions. Some even have more than 250 extreme heat days compared with that at present. The result of ssp585 is generally similar to that of ssp370 but slightly higher in some areas of North America, South America and Australia.

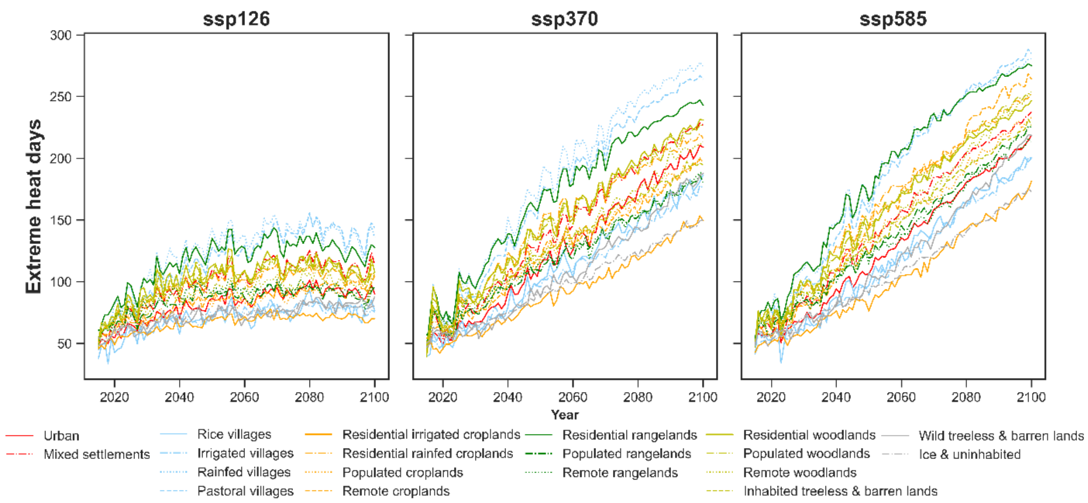

Figure 3: frequency of extreme heat of each anthrome. The frequency of this figure is the mean value of frequency in five GCMs from 2015 to 2100 and uses 90th percentile daily air maximum temperature as the threshold. The vertical axis represents the number of extreme heat days per year.

The frequency of extreme heat for each anthrome increased overall with a prolonged period but displayed a slight difference in the frequency rate for specific anthrome. Extreme heat days for each anthrome had a similar increasing trend with slightly different speeds at the first 40 years (Fig 3). For ssp126, extreme heat days increased stably until 2050, then the frequency of extreme heat days stabilized with minor fluctuations from 2050 to 2100. The mean frequency of extreme heat was limited to less than 150 days for all anthromes in ssp126. Different results were observed in ssp370 and ssp585, and those two scenarios had similar results with a continuously increasing trend until the end of the 21st century. Extreme heat days exceeded 150 days for all anthromes in both scenarios, and in ssp585 were slightly larger than in ssp370, consistent with the observed results in Fig 2. Besides the difference among future scenarios, extreme heat days for different anthromes are slightly different with a similar trendline. For example, irrigated villages and rainfed villages were both the sub-village-system under anthrome classification. However, the extreme heat days of rainfed villages reached about 140 days per year in 2100 in ssp126, while extreme heat days of irrigated villages were only 70 days, half that of rainfed villages. The main reason for such a huge difference might be the spatial distribution of these two anthromes and the unequal global increasing temperature. As is shown in Fig A-2, a large area of rainfed villages is located in Africa, where extreme heat days increase quicker than in other regions of the world.

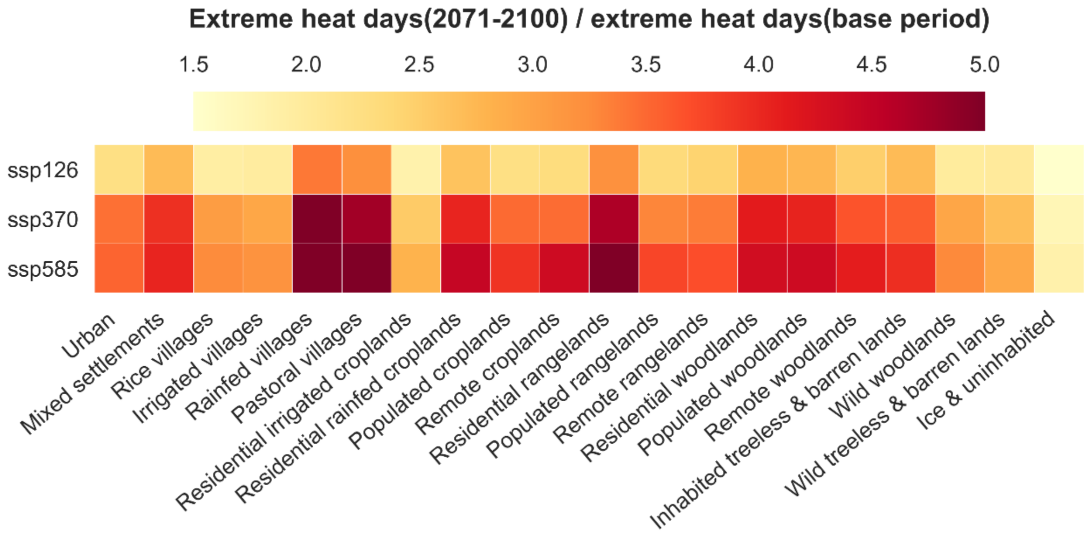

Figure 4: extreme heat days increase ratio, mean extreme heat days from 2071 to 2100 divided by mean extreme heat days of the base period (1985 to 2014) to represent the growth rate of extreme heat events in each anthrome compared with that of the base period.

The frequency of extreme heat rose at different rates for different anthromes under different scenarios (Fig 4). For ssp126, there was an increase of 3 times of extreme heat days for most anthromes except for rainfed villages, residential rangelands, and pastoral villages. While, for the other two scenarios, extreme heat days increased more than three times for nearly all anthromes, except for residential irrigated croplands and Ice & uninhabited. There was no significant difference between ssp370 and ssp585, which was consistent with the former results (Fig 2 and Fig 3). For high population density anthromes such as rained, pastoral, and residential villages, extreme heat days increased significantly compared with ssp126, leading to more pressure than other anthromes.

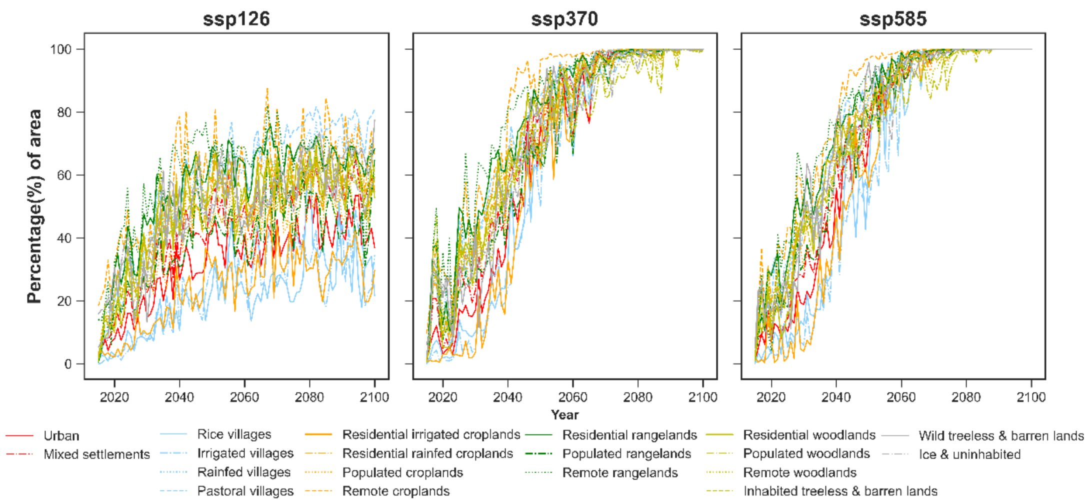

Figure 5: Percentage of the area that will experience more extreme heat events than that of base period(1985-2014) for each anthrome. The percentage of the area is the total area of each anthrome divided the area experiencing more extreme heat events (area where extreme heat days > 36.5 days per year). This figure uses the 90th percentile daily maximum air temperature as a threshold and calculates the mean frequency of five GCMs. The detailed dynamic of land use(cover) is in the appendix(Fig A-(4 to 7)

In addition to extreme heat days, a novel concept, ‘area with more extreme heat’, was also introduced (Fig 5), representing the regions influenced by extreme heat in the future. The 90th percentile daily air maximum temperature was selected as the threshold, indicating that the extreme heat days of the base period were 36.5 days per year on average. We defined that if the frequency of extreme heat was larger than 36.5 days, that area (grid) experienced more extreme heat events than the base period. In ssp126, the area with the more extreme heat of each anthrome increased quickly for the first 30 years, then it stopped rising and stabilized for the last 50 years. For most anthromes, 40% to 60% of the area underwent more extreme heat events than the base period, indicating that from that time, half of the regions in most anthromes were influenced by more frequent extreme heat events. There are a few anthromes such as rice villages with less area(<30%), experiencing more heat in the future. And there were also some anthromes such as remote cropland and pastoral villages with more area(>60%) influenced by more extreme heat, consistent with the results above (Fig 3 & 4). The results of ssp370 and ssp585 were similar. The area influenced by extreme heat kept increasing rapidly until the middle of the 21st century. The year 2060 was a signal, representing that all areas in each anthrome experienced more heat events in ssp370 and ssp585.

3.2 Human health

Frequency of heat days

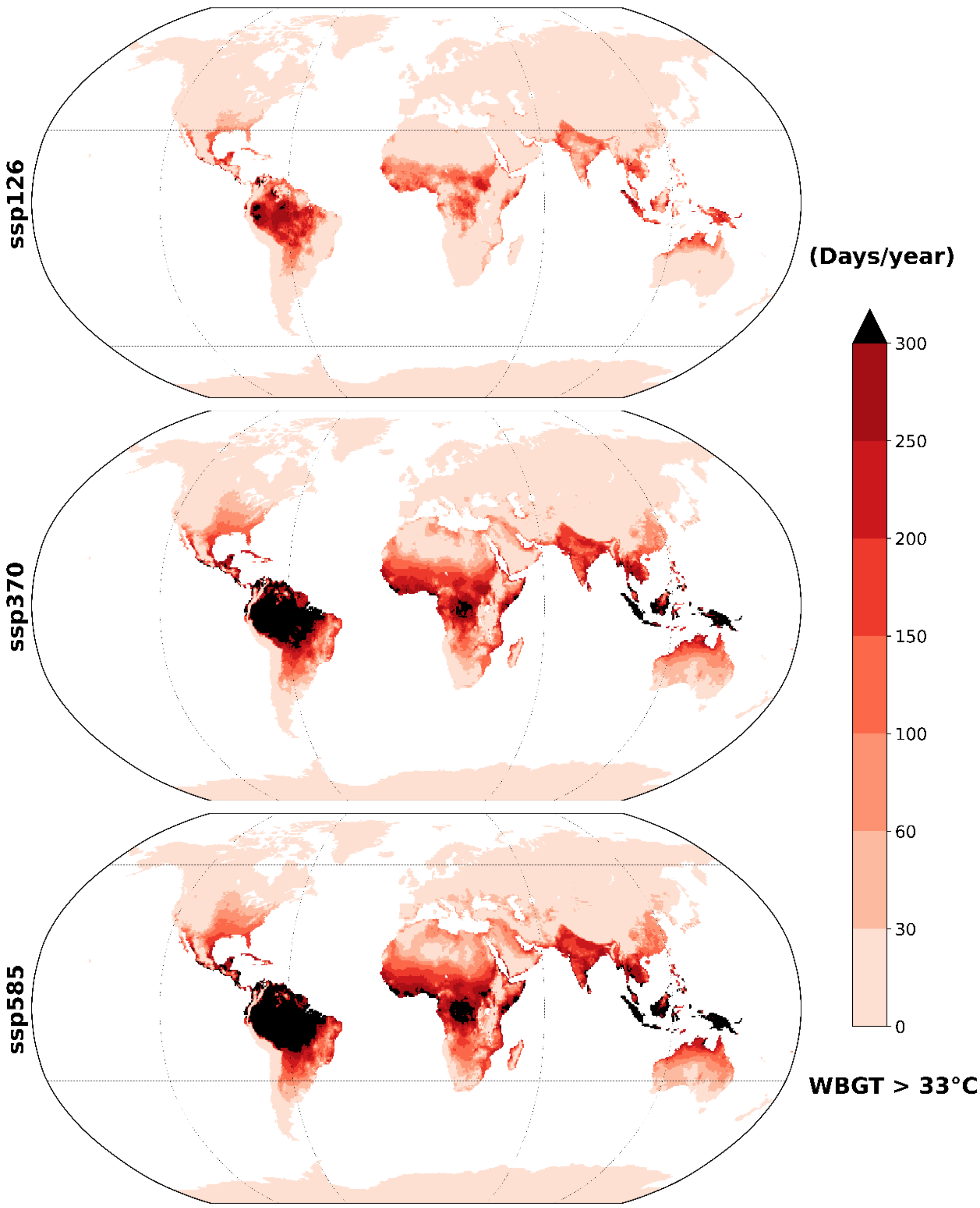

Figure 6: spatial distribution of frequency of extreme heat in terms of human health (WBGT = 33°C) at 2100, mean values of five CGMs.

For human health, the popular and widely used heat indicator: WBGT was adopted as a heat threshold to count the yearly extreme heat days. As observed in Fig 6, most extreme heat events in terms of human health took place in tropical and sub-tropical areas. For other regions, the extreme heat days were limited to less than 30 days in 2100 under all future scenarios.

For ssp126, India, south of China, Southeast Asia, southern North America, and most regions in South America experienced more extreme heat events than other regions, with more than 60 days of extreme heat in 2100. In a few areas of South America, WBGT exceeded the threshold for most time of the year (frequency > 200 days). Extreme heat days in ssp126 were overall limited to less than 200 days in most regions.

However, there was a significant difference between ssp126 and the other two scenarios. The area prone to suffer from frequent heat events (frequency > 100 days) expanded, and the frequency of extreme heat events also increased globally. Especially in South America and Southeast Asia, WBGT exceeded the threshold for nearly all days in one year (frequency > 300 days). And there were no obvious differences between ssp370 and ssp585. Only a slight expansion in area or increase in frequency in a few regions such as Africa were observed between ssp370 and ssp585.

Population exposure to heat

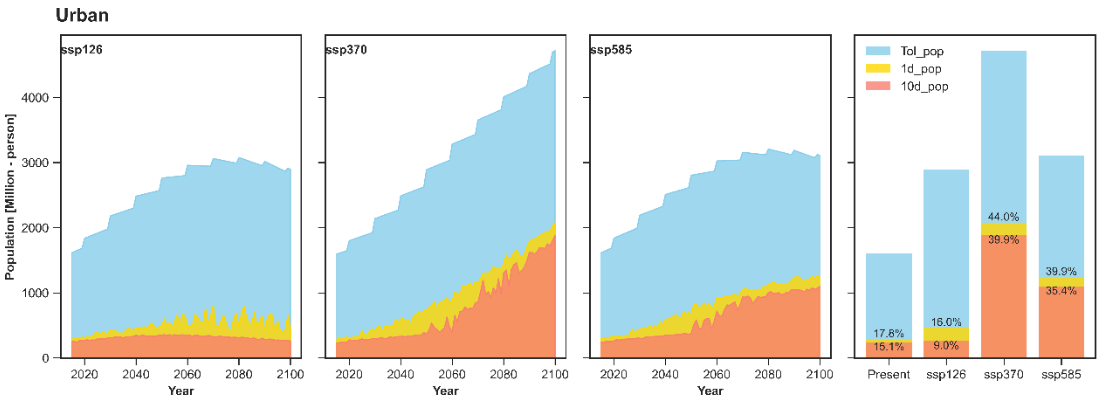

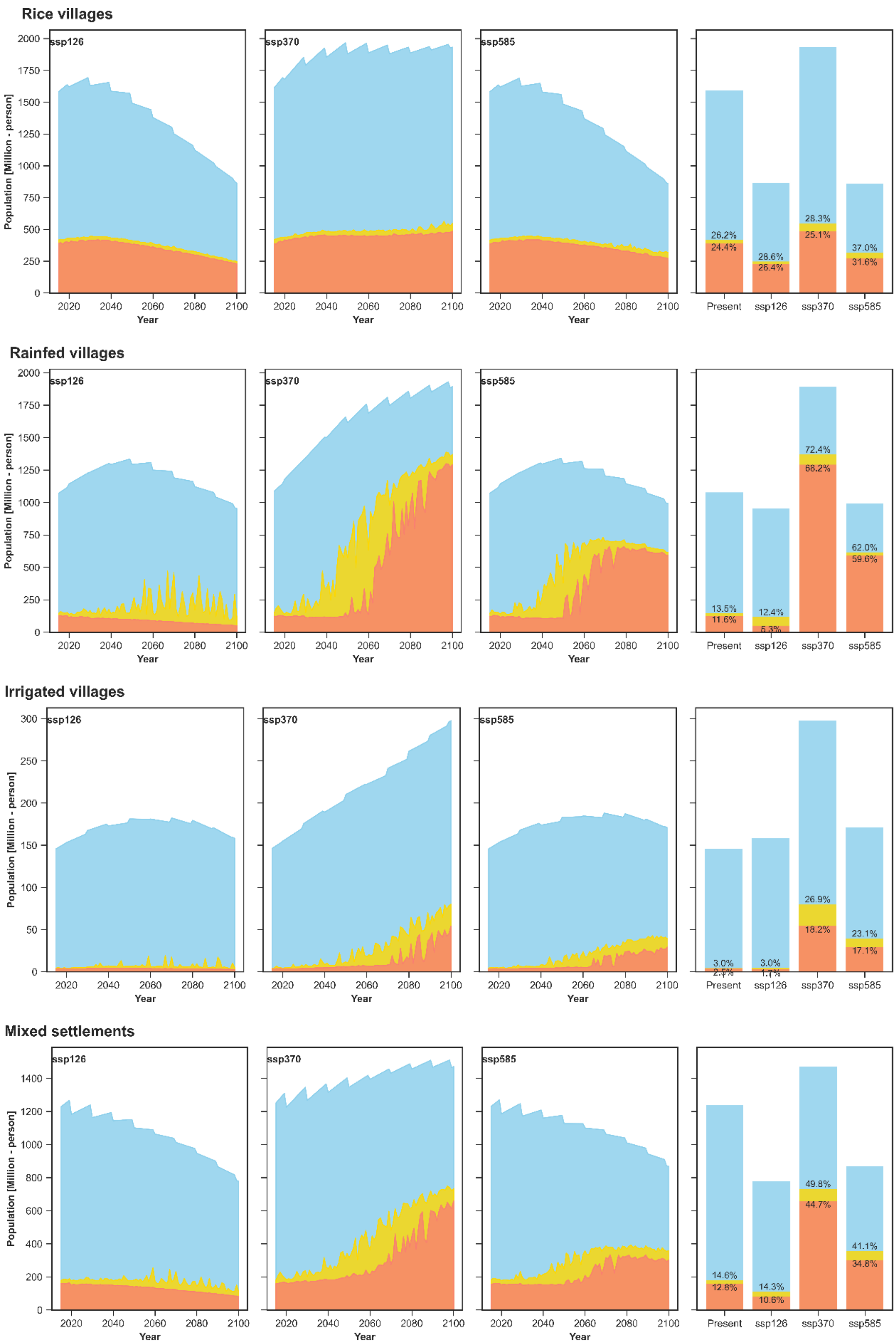

Rice villages
Rainfed villages
Irrigated villages
Mixed settlements
Population [Million - person]
Year
ssp126
ssp370
ssp585
Present
26.2%
24.4%
28.6%
26.4%
28.3%
25.1%
37.0%
31.6%
13.5%
11.6%
12.4%
5.3%
72.4%
68.2%
62.0%
59.6%
3.0%
2.5%
3.0%
1.7%
26.9%
18.2%
23.1%
17.1%
14.6%
12.8%
14.3%
10.6%
49.8%
44.7%
41.1%
34.8%

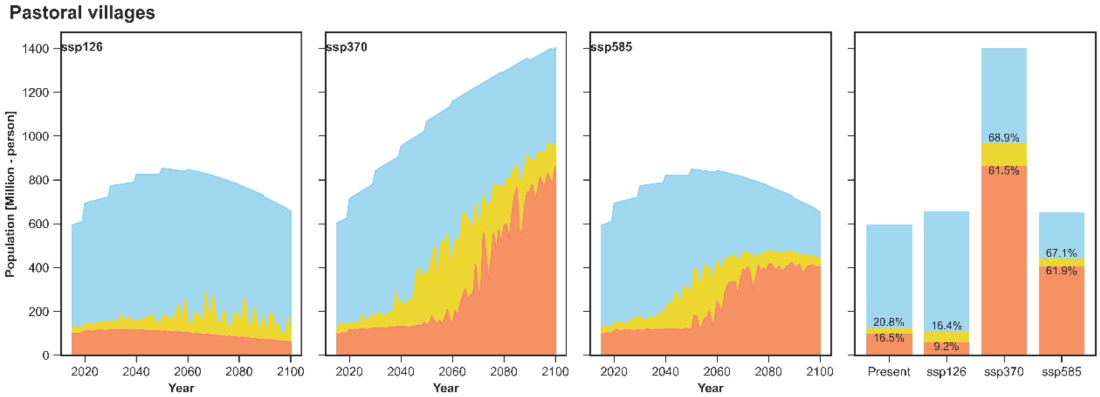

Figure 7: population exposed to extreme heat in six high-density anthrome from 2015 to 2100 (WBGT = 30°C). The blue part represents the total amount of population in each anthrome, the yellow part refers to the population exposed to heat > 1 day, and the orange parts represent the population exposed to heat > 10 days. The bar chart represents the percentage of the population exposed to heat in 2100.

To estimate how many populations would be exposed to extreme heat events in the future, six high-density anthrome areas were chosen: (1) urban (2) rice villages (3) rainfed villages (4) irrigated villages (5) mixed settlements (6) pastoral (Fig A-1). For these six anthromes, the total population of each scenario varied compared with that at present (blue part in Fig 7). Ssp370 had faster population growth while the population of ssp126 and ssp585 had a similar trend over time, increasing in the first 40 years and then decreasing until 2100. The perturbation every decade results from future land use and cover change for every 10 years in integrated assessment models (IAMs)

Population exposure (%) to extreme heat was also different among those anthromes. At present, 26% population was exposed to heat in rice villages, while irrigated villages had only 3% population influenced by extreme heat events. The main reason to explain such a huge difference is the spatial distribution of these anthromes worldwide, and anthromes located near the equator might be more likely to be attacked by extreme heat.

For ssp126, the population exposed to heat stabilized over time for all anthromes, even with a mild decrease in rice villages, mixed settlements, and pastoral villages. For ssp370, the population exposed to heat remained stable for the first three decades. It then increased more or less after 2050 for all anthromes except rice villages, which had a stable population exposed to heat for all these three scenarios over time. The population exposed to the heat of urban, rainfed villages, mixed settlements, and pastoral villages increased faster than in other anthromes, with 45% to 72% population exposed to extreme heat in 2100.

Obvious differences were observed between ssp370 and ssp585 since 2060. For most anthromes, the population exposed to heat events of ssp370 increased faster than that of ssp585. While in ssp585, population exposure to heat rose for the first 60 years and then stabilized after 2080 in most anthromes, which might result from the difference in total population growth between ssp370 and ssp585 of each anthrome. In summary, the change in population exposure to extreme heat was the interaction of changes in the frequency of extreme heat and population dynamics over time.

In addition to humans exposed to heat > 1 day, populations exposed to heat > 10 days are also presented (Fig 7, orange part). Most populations exposed to heat > 1 day were also prone to suffer from more than 10 days' extreme heat per year in all high population density anthromes. It indicated that extreme heat events for human health occurred frequently and intensively in certain regions (tropical and sub-tropical areas) of the world (Fig 6).

3.3 Crops

Frequency of extreme heat

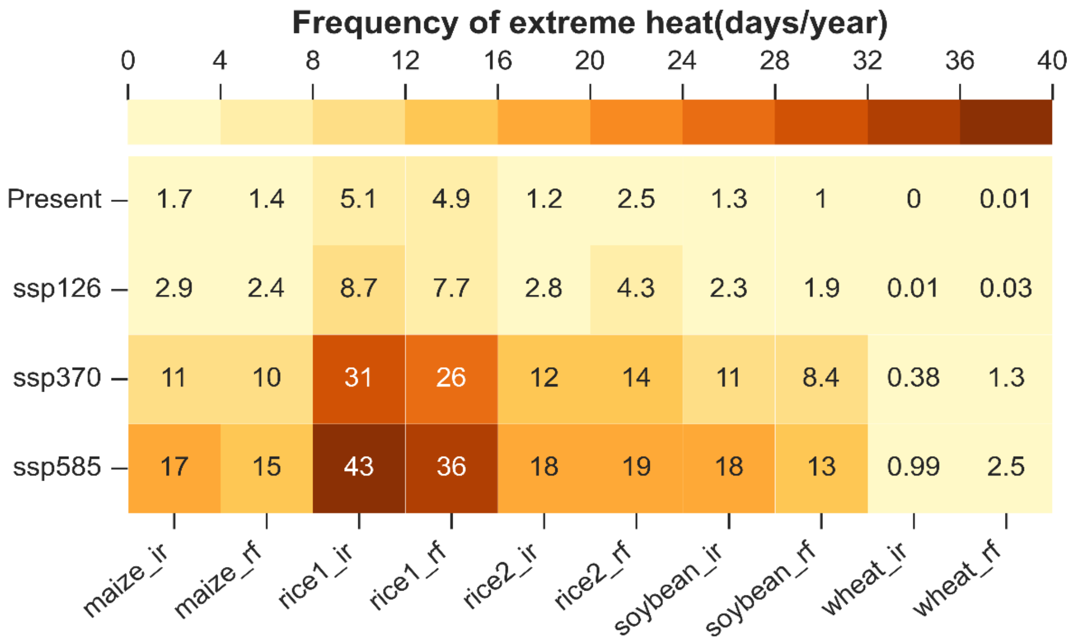

Figure 8: frequency of extreme heat for 4 major crops, ir means irrigation, and rf means rainfed. Present in the y-axis means the year 2015, and three SSPs followed refer to 2100 in different future scenarios. The x-axis represents 5 major crops separated by rainfed and irrigation systems. The colour and values in each cell refer to the mean extreme heat days in the corresponding year (present: 2015; ssp126,ssp370,ssp585: 2100). This figure uses mean values of frequency in five GCMs, the frequency over time is in the appendix (figure A-12).

As Fig 8 shows, the extreme heat days ranged from 0 to 5 days for different crops at present. Among those crops, rice had longer heat days than other crops because a lower threshold was selected for rice (32°), and large rice harvested area was planted in ‘hot’ regions like Asia, Africa and South America (Fig A-3). For wheat, the extreme heat days were much smaller than other crops because the winter wheat calendar was chosen in this research, excluding some hot days in summer.

The frequency of extreme heat events of four crops increases more or less in all future scenarios. In ssp126, extreme heat days nearly doubled for most crops, while in ssp370 and ssp585, extreme heat days increased much faster than in ssp126. Especially in ssp585, the extreme heat days increased more than 10 times than the present for most crops, indicating that crops would face poor growing conditions in such an extreme scenario. Among those crops, rice was most influenced by extreme heat, while wheat was least influenced. Rice season 1 has the largest extreme heat days (43/36 days), while rice2 only has 18/19 days in 2100, half of rice1. It might result from different growing seasons between rice 1 and rice 2. Although the extreme heat days of wheat increased a lot compared with the present, it only has 0.99/2.5 days, which was much smaller than other crops.

Area influenced by extreme heat

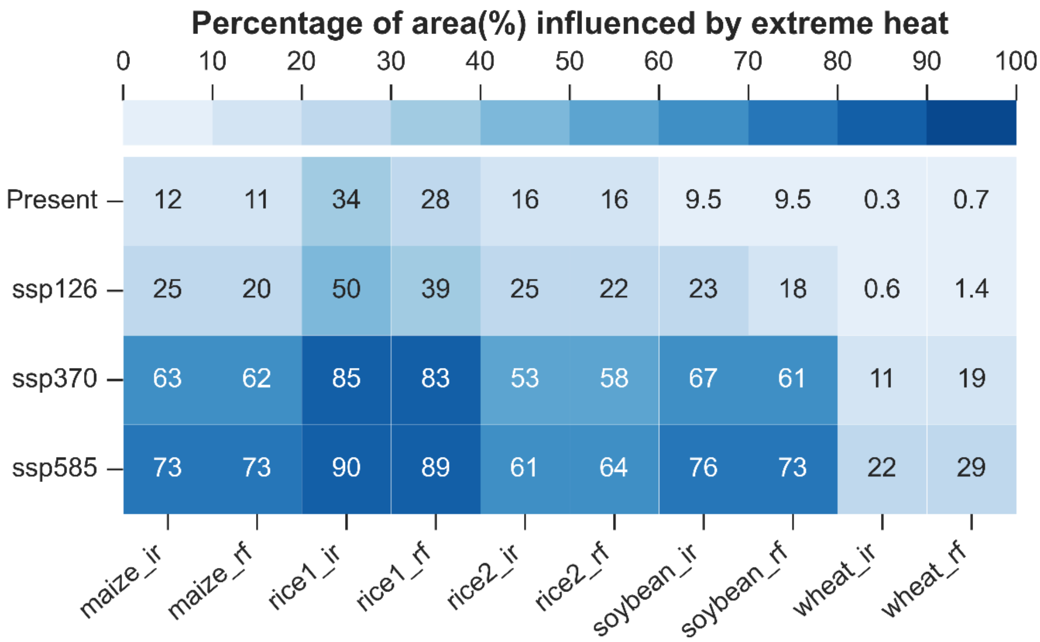

Figure 9: Percentage of the area(%) that was influenced by extreme heat for 4 major crops. Present in the y-axis means the year 2015, and three SSPs followed refer to 2100 in different future scenarios. The x-axis represents 5 major crops separated by rainfed and irrigation systems. The value in each grid was calculated by dividing the area that experienced extreme heat (extreme heat day > 0) by the total crop harvest area.

Fig 9 showed the percentage of the area (%) influenced by extreme heat, representing the scale of the extreme heat events. At present (2015), most crop areas (>70%) were not affected by extreme heat events. Among those crops, maize, soybean, and wheat had less than 10% area that was influenced by extreme heat. Rice 1 and 2 had more than 16% and 28% of the area experiencing extreme heat events, similar to the result of Fig 8.

The area influenced by extreme heat also increased under different future scenarios. For ssp126, the area rose 1 to 2 times than that at present, while the area increased much faster in the other two scenarios. The results of ssp370 and ssp585 were similar, with only a minor increase in ssp585. In ssp585, rice, maize, and soybean had more than 60% of areas affected by extreme heat events, while wheat only had less than 30% of areas influenced. Rice 1 was worst affected, with about 90% area influenced by extreme heat for rainfed and irrigation systems, whereas rice 2 only had 60% area affected. Wheat had the least areas affected by extreme heat than other crops, less than 20% in ssp585. In general, the result of the area influenced by extreme heat is similar to the result of extreme heat days for each crop in Fig 8, indicating that crops with higher extreme heat days tended to have more areas influenced by extreme heat. It revealed that the frequency and scale of extreme heat increased in the future.

4. Discussion

4.1 Extreme heat frequency and scale

This research comprehensively quantifies future extreme heat under different scenarios regarding human health, crops, and anthrome. We mainly focus on two indicators that describe the extreme heat: (1) extreme heat days (for anthrome, human health and crop parts) (2) area affected by extreme heat (for anthrome and crops parts).

The extreme heat days for each anthrome under ssp126, ssp370, and ssp585 have a similar increasing trend for the first two decades, indicating little space for climate mitigation strategies. But for the coming decades, the extreme heat days vary obviously between three scenarios. The frequency of ssp370 and ssp585 has a similar increasing trend while it is different for ssp126, which remains stable after 2060. The area with more extreme is applied to this research part, indicating the scale of extreme heat events within a year. The result is consistent with the frequency of extreme heat for these three scenarios. Three scenarios have a similar increasing trend for the first 20 years, and then ssp126 remains stable while the other two scenarios continue increasing. For ssp370 and ssp585, The year 2060 is a signal, indicating that the whole terrestrial system will face more extreme heat weather than the base period.

This research adopted the popular and widely used heat index, wet bulb globe temperature, for human health. Extreme heat events for humans mainly occur in tropical and subtropic areas because of higher temperatures and humidity than in other regions. Especially for south America, Africa, and Southeast Asia, their daily climate conditions will easily exceed the WBGT thresholds. For most populated anthromes, the population exposed to extreme heat decreases slightly at the end of the 21st century in ssp126. While for the other two scenarios, the population exposed to heat keeps increasing in ssp370 and starts to decrease after 2050 in ssp585. Population exposure to heat is not only the result of climate change but also relates to socioeconomic elements such as population growth and land-use change.

Scholars made efforts to quantify extreme heat events regarding WBGT in the past and future. Tuholske et al. (2021) quantified extreme heat events using hourly observational climate databases for the past 30 years. However, future projections of extreme heat using WBGT have to be developed yet. Li et al. (2020) projected future assessed future WBGT as a function of increasing global mean surface air temperature, but it only considered RCP8.5, ignoring other future scenarios. This research adopted NOAA's algorithm to estimate extreme heat under more future scenarios. However, there is a significant difference between this research and Tuholske's result. More than 90 billion 'population-days' will be exposed to extreme heat, while there are only about 40 billion 'population-days' in this research in 2015 for the urban area (Fig A-10), and it mainly results from the definition of the urban area. Global Human Settlement Layer Urban Centre Database (GHS-UCDB) was used in Tuholske's study, and more than half the population lived in the urban area. However, the urban area was re-defined in anthrome classification in a stricter rule, and only 1.6 billion population lived in urban anthrome in 2015 (Ellis et al., 2021; Florczyk et al., 2019). And other factors such as different climate database input and estimation methods can also cause inconsistency.

For the crop part, the frequency of extreme heat days increases under various scenarios as well. But there are distinguished increasing trends among those crops because crops have different planting and growing seasons (Fig A-12), such as winter wheat, whose growing season might exclude some hot days in summer. And rice 2 will also experience less heat than rice 1 due to different planting seasons. Those four major crops will face more frequent and intensive extreme heat events than the present. However, due to different growing seasons, heat tolerance, and spatial distribution, the impact of extreme heat events on those 4 crops makes a big difference, leading to uncertain threats to food security in the future. Therefore, climate adaptation and mitigation strategies should consider variations in the impacts of extreme heat events on different crops. Our results showed no significant difference between rainfed and irrigation systems within various crops. The rainfed systems deserve more attention because frequent extreme heat events are always associated with drought (Fahad et al., 2017). Besides the direct impacts of extreme heat, water scarcity can also threaten crops in rainfed systems. The area(%) influenced by extreme heat is less than 16% for most crops except rice 1. For ssp126 at 2100, the area has increased less than doubled compared with the present. While for ssp370 and ssp585, nearly more than 60% area will experience extreme heat at 2100 for all crops except for winter wheat. In the latest Global Gridded Crop Model Intercomparison Phase 6, crop models like LPJmL improved their behaviour by considering extreme heat (Jägermeyr et al., 2021). However, most crop models still underestimate yield responses to extreme heat and drought (Heinicke et al., 2022). Therefore, this research conducted the crop part from a land perspective, not adopting crop production projection in the future.

4.2 Data input uncertainty and threshold sensitivity

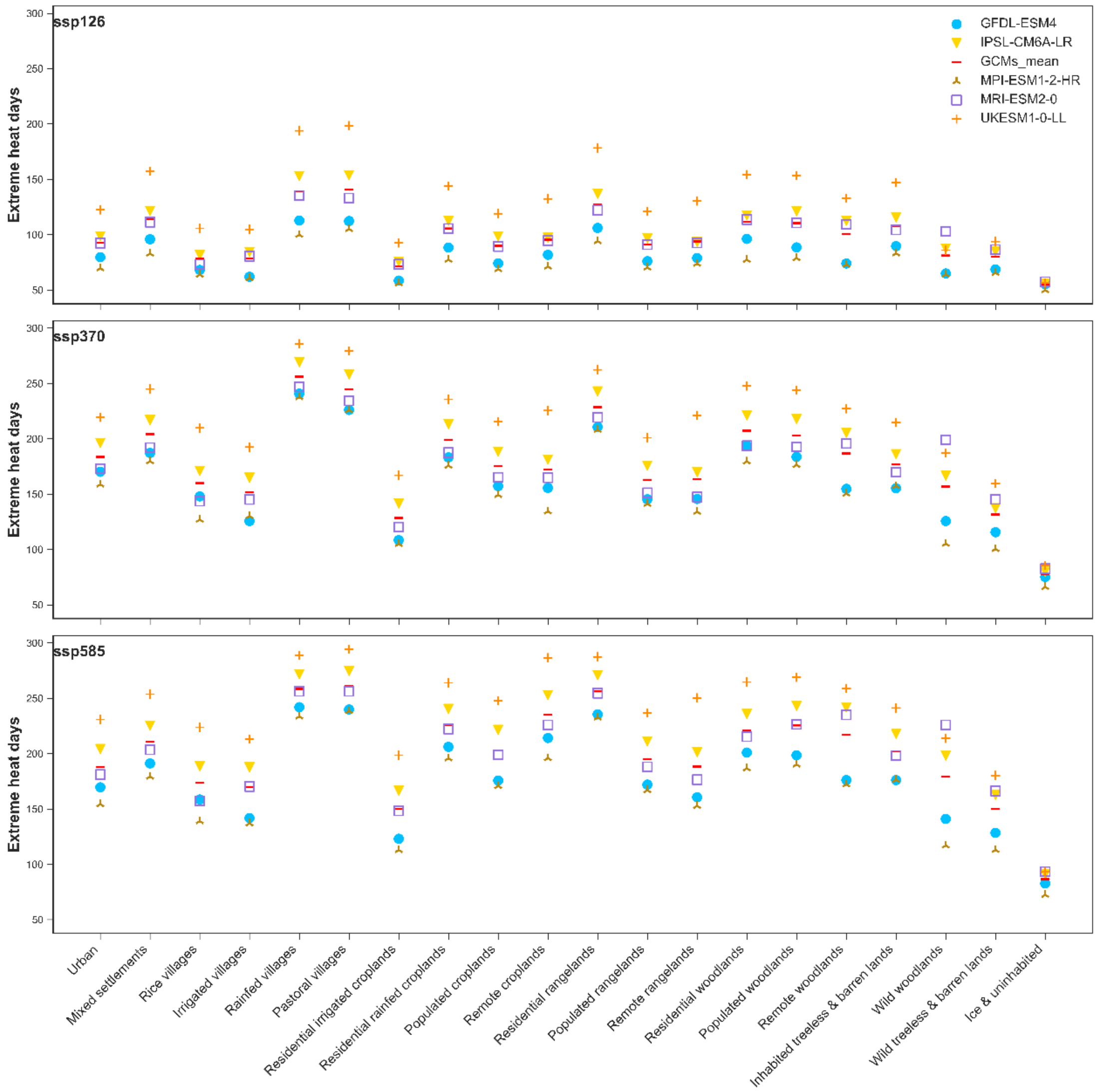

Figure 10: uncertainty of climate forcing models. The five climate forcing databases((1) GFDL-ESM4, (2) IPSL-CM6A-LR, (3) MPI-ESM1-2-HR, (4) MRI-ESM2-0, and (5) UKESM1-0-LL) were analyzed separately and mean value of climate ensemble was also calculated (solid red line) to explore the uncertainty.

As Fig 10 showed, the result of UKESM1-0-LL and IPSL-CM6A-LR have a clear difference compared with the other three models, especially for UKESM1-0-LL, whose simulation causes more than 50 days of frequency higher than other models for nearly all anthromes. This is consistent with the TCR and ECS values of those climate models, where UKESM1-0-LL and IPSL-CM6A-LR have higher values of TCR and ECS than others. Three low-sensitivity GCMs have similar results because their TCR and ECS are close to each other. For most future scenarios and anthromes, the mean value of ensemble is located in the middle of that individual analysis of each GCM, which helps reduce uncertainty compared with using only one model.

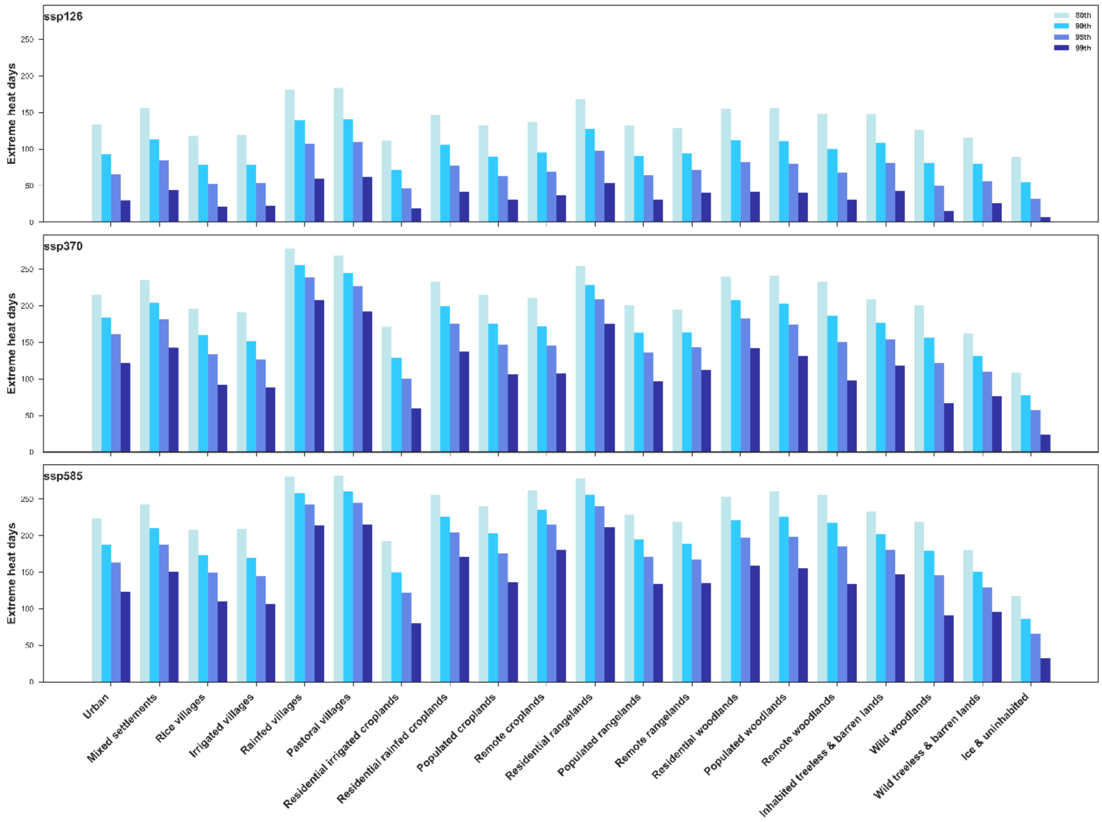

Figure 11: uncertainty of temperature thresholds (80th, 90th, 95th, 99th), mean values of extreme heat days of five GCMs for all future scenarios (ssp126, ssp370, ssp585) at 2100.

For the anthrome part, a relative threshold strategy was developed to quantify extreme heat events for anthromes. 90th percentile daily maximum temperature of the base period was selected as the baseline (Chen et al., 2020; Sulikowska & Wypych, 2020). However, the frequency of extreme heat might be sensitive to different thresholds. Fig A-11 showed that extreme heat days increase with decreasing thresholds in all anthromes. For ssp370 and ssp585, some areas such as South America and southern Africa have more than 300 days when the 80th percentile threshold was selected, indicating that nearly all daily air maximum temperatures exceed the thresholds at the end of the 21st (Fig A-11). For the threshold of 99th, the frequency increase much faster from ssp126 to ssp370 and ssp585 than in other thresholds because the frequency in some region might reach the boundary (more than 300 days per year) quickly when choosing other low-temperature thresholds.

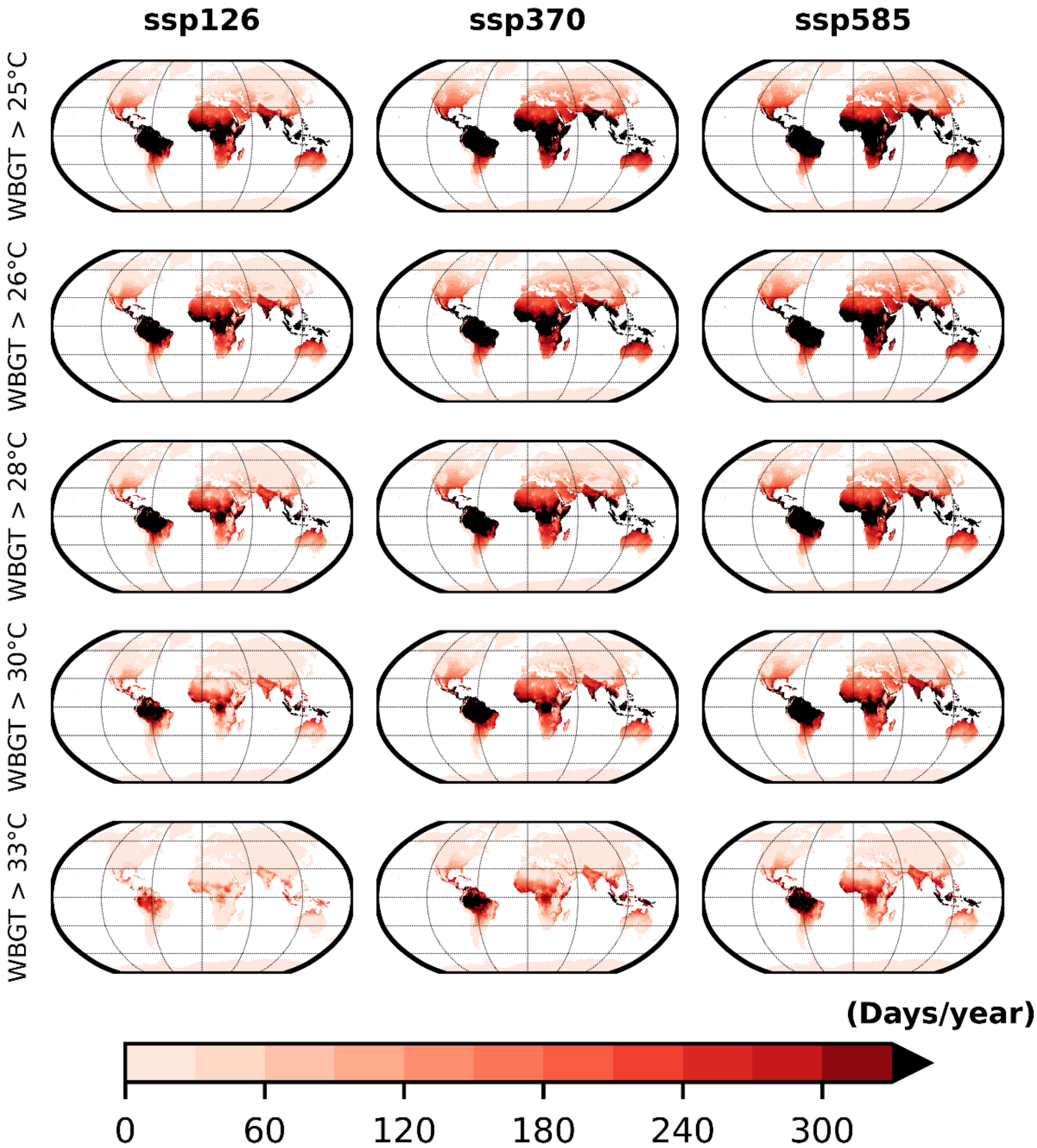

Figure 12: Changes of five WBGT thresholds (25°C, 26°C, 28°C, 30°C, 33°C), mean values of extreme heat days (WBGT) of five GCMs in 2100.

Five WBGT thresholds are selected in this research, representing different metabolic rates. Fig 12 indicates the frequency of extreme heat days at five different WBGT thresholds. For all scenarios, the extreme heat days decrease with the increasing thresholds. There is no clear difference between WBGT = 25°C and 26°C for most regions under three SSPs. Most regions in the tropic area have extreme heat over 300 days, while most subtropic areas have more than 180 extreme heat days. For WBGT > 28°C, the obvious difference can be observed between ssp126 and ssp370, ssp585. Some areas, such as Africa, will experience less extreme heat in ssp126 than the other two SSPs. WBGT = 30°C is regarded as a threat to human health and this research chose it as the baseline (Tuholske et al., 2021). WBGT > 33°C is an extreme condition for human health, and there is an obvious difference between ssp126 and ssp370.

4.3 Limitation

The limitations of this research will be discussed separately in three research parts. There are many ways to define extreme heat events based on climate parameters and research objectives (Horton et al., 2016). Absolute temperature and percentiles were always used to determine the threshold (Horton et al., 2016). Firstly, for the anthrome part, the relative temperature threshold method was adopted to extract the base period's 90th percentile daily maximum temperature to determine the extreme heat threshold. However, it successfully investigated if a specific area will experience more high-temperature days than the base period, but whether the threshold of each grid is 'extreme' for local anthrome is unknown. For example, in some cold urban anthrome, the 90th percentile temperature is less than the human limit. Using the relative threshold in this helps give consistent and global research on extreme heat but lacks respect to local and regional anthrome. More detailed and small-scale research is needed. This research used the present as the reference period to quantify the extreme heat on anthrome in the future. The reference period in other research, such as the IPCC report, pre-industrial, was always chosen as the base period. Therefore, it is also possible to extend the period to pre-industrial.

For human health, an international standard (Iso, 2017) was adopted to quantify the extreme heat days in populated areas. There are limitations to estimating the daily WBGT. WBGT consists not only of air temperature and relative humidity but also of wind speed, sun angle, and other climate variables. Due to the data availability, an empirical formula was applied to this research to estimate daily WBGT (Liljegren et al., 2008). It might bring deviation and uncertainty to the results. The second limitation is the climate input database itself because the historical climate database provides hourly climate data while the ISIMIP ensemble only offers daily climate variables, which might lead to uncertainty. For example, when the air temperature reaches the maximum temperature at a day, the relative humidity reduces to the minimum of that day (Tuholske et al., 2021). The relative humidity in this research is overestimated, causing deviation to the results, especially in high humidity area like south America, whose relative humidity is always bigger than 80%.

The limitations mainly come from the assumptions and threshold determination for the crop part. Firstly, a crop calendar was adopted in this research, which provided the planting date and growing season of those 4 major crops. However, this calendar is suitable for present and historical research but not for future situations. The fixed planting date and growing season might not be consistent with a warming future. Secondly, fixed land use for those crops in 2015 was used for those crops, ignoring the different future socio-economic scenarios because of data limitations. Except for SSP1, the cropland of the other 4 SSPs will increase more or less at the end of the 21st century (Riahi et al., 2017), causing inconsistency with this research. Besides, a simple and certain air temperature was selected as the heat stress threshold for crops. However, different growing phases usually have different heat tolerance and response to extreme heat. Distinguishing the different growing phases of each crop and using different absolute temperature thresholds can help reduce the uncertainty of the quantification.

4.4 Outlook

This research gives a comprehensive and global quantification of extreme heat in the terrestrial system. It is always unsatisfactory and uncertain in methodology and data source. I will first provide some ideas for improving them and then introduce future research directions.

This research has chosen three future climate-socioeconomic scenarios (ssp126, ssp370, and ssp585) to explore the frequency and scale of extreme heat events in the future. However, the latest report indicates that RCP8.5 is too extreme and unrealistic (Vuuren, 2022). Therefore, the most extreme scenarios might be given up for the future direction. For human health, this research simply used extreme heat days instead of heat waves, and the definition of heat waves was not consistent globally. Future work might focus on developing a consistent and comprehensive international standard for heat stress in human health. For the crop part, some projects, such as Harmonization of Global Land Use Change and Management (LUH2), provided future land use and made efforts to subdivide cropland into five functional crops (Hurtt et al., 2020). However, it failed to provide dynamic and specific crop growing areas under future scenarios. Therefore, other land use databases, such as the IMAGE framework, can be used in this research to reduce uncertainty. In addition to the direct impact of extreme heat on crops, other hazards such as drought caused by extreme heat should also be considered.

5. Conclusion

This research quantified future extreme heat by combining different future scenarios and anthrome perspectives. Relative and absolute extreme heat threshold strategies were adopted in this research regarding the land system, human health, and major crops.

The results for anthrome indicated that the frequency of extreme heat events would increase more or less in three future scenarios. For the period before 2050, these three scenarios have a similar increasing trend. After 2050, the frequency of ssp126 remains stable while the other two scenarios continue to increase at the end of the 21st century. As for the area influenced by extreme heat, three scenarios also have a similar increasing trend before 2040. Then after 2060, all anthromes will experience more extreme heat events than the base period in ssp370 and ssp585.

The extreme heat events for human health mainly will occur in the world's tropical and subtropical regions. The frequency of extreme heat days in all scenarios will increase to some degrees with time. Population exposure in ssp126 to heat is close to that of the present. In ssp370 and ssp585, 23%-72% of the population in different anthromes will be exposed to heat at the end of the 21st century.

For the crop part, four major crops were selected and analyzed in this research to quantify the frequency and scale of extreme heat events. The frequency of extreme heat events of four crops increases more or less in all future scenarios. In ssp126, the extreme heat days almost doubled for most crops, while in ssp370 and ssp585, the frequency increases much faster, especially for ssp585, the frequency of extreme heat increases about 10 times for all crops. At present, most crop areas (>70%) are not affected by extreme heat events. For ssp126, the area increases 1 to 2 times than that at present, while the area increases much faster in the other two scenarios. Among those crops, rice 1 will be most influenced by extreme heat events, while winter wheat will be least affected.

We provide a comprehensive and global quantification of extreme heat events considering the land system, human health, and food security. There is no surprise that extreme heat events increase in all future scenarios, and the scale of extreme heat will also expand. But the effects of extreme heat events on different research objectives make a difference due to the variation of spatial distribution, extreme heat definition, and growing season(crop). Therefore, more detailed and relevant research is needed to understand extreme heat regarding land-atmosphere interaction better. And appropriate climate adaptation and mitigation strategies are also necessary to cope with more frequent and intensive extreme heat events in the future.

6. Reference

Allan, R. P., Hawkins, E., Bellouin, N., & Collins, B. (2021). IPCC, 2021: summary for Policymakers.

Australian Bureau of Agricultural and Resource Economics and Sciences. (2010). Cropping calendars for natural resource management regions of Australia.

Baboo, S. S., & Devi, M. R. (2010). An analysis of different resampling methods in Coimbatore, District. *Global Journal of Computer Science and Technology*.

Barriopedro, D., Fischer, E. M., Luterbacher, J., Trigo, R. M., & García-Herrera, R. (2011). The Hot Summer of 2010: Redrawing the Temperature Record Map of Europe. *Science*, *332*(6026), 220-224. https://doi.org/doi:10.1126/science.1201224

Basu, R., & Samet, J. M. (2002). Relation between Elevated Ambient Temperature and Mortality: A Review of the Epidemiologic Evidence. *Epidemiologic Reviews*, *24*(2), 190-202. https://doi.org/10.1093/epirev/mxf007 %J Epidemiologic Reviews

Berkman, P. A., & Young, O. R. (2009). Governance and Environmental Change in the Arctic Ocean. *Science*, *324*(5925), 339-340. https://doi.org/doi:10.1126/science.1173200

Bernard, T. E., & Iheanacho, I. (2015). Heat index and adjusted temperature as surrogates for wet bulb globe temperature to screen for occupational heat stress. *Journal of Occupational and Environmental Hygiene*, *12*(5), 323-333.

Budd, G. M. (2008). Wet-bulb globe temperature (WBGT)--its history and its limitations. *J Sci Med Sport*, *11*(1), 20-32. https://doi.org/10.1016/j.jsams.2007.07.003

Budd, G. M. (2008). Wet-bulb globe temperature (WBGT)—its history and its limitations. *Journal of Science and Medicine in Sport*, *11*(1), 20-32.

CDC. (2018). *Heat Stress, Acclimatization*. Retrieved May, 24th from https://www.cdc.gov/niosh/topics/heatstress/acclima.html

Chen, J., Liu, Y. J., Pan, T., Ciais, P., Ma, T., Liu, Y. H., . . . Penuelas, J. (2020). Global socioeconomic exposure of heat extremes under climate change. *Journal of Cleaner Production*, *277*, Article 123275. https://doi.org/10.1016/j.jclepro.2020.123275

Clements, F. (1916). The development and structure of biotic communities. *J. Ecol*, *5*, 12-21.

CONAB. (2019). *Calendário de Plantio e Colheita de Grãos no Brasil 2019*

Council, A. (2021). EXTREME HEAT: The Economic and Social Consequences for the United States. *Adrienne-Arsht Rockefeller Foundation Resilience Center*.

Ellis, E. C., Gauthier, N., Goldewijk, K. K., Bird, R. B., Boivin, N., Díaz, S., . . . Watson, J. E. M. (2021). People have shaped most of terrestrial nature for at least 12,000 years. *Proceedings of the National Academy of Sciences*, *118*(17), e2023483118. https://doi.org/doi:10.1073/pnas.2023483118

Ellis, E. C., Klein Goldewijk, K., Siebert, S., Lightman, D., & Ramankutty, N. (2010). Anthropogenic transformation of the biomes, 1700 to 2000. *Global Ecology and Biogeography*, *19*(5), 589-606. https://doi.org/https://doi.org/10.1111/j.1466-

8238.2010.00540.x
Ellis, E. C., & Ramankutty, N. (2008). Putting people in the map: anthropogenic biomes of the world. *Frontiers in Ecology and the Environment*, *6*(8), 439-447. https://doi.org/10.1890/070062
Enayati, M., Bozorg-Haddad, O., Bazrafshan, J., Hejabi, S., & Chu, X. (2020). Bias correction capabilities of quantile mapping methods for rainfall and temperature variables. *Journal of Water and Climate Change*, *12*(2), 401-419. https://doi.org/10.2166/wcc.2020.261
Eyring, V., Bony, S., Meehl, G. A., Senior, C. A., Stevens, B., Stouffer, R. J., & Taylor, K. E. (2016). Overview of the Coupled Model Intercomparison Project Phase 6 (CMIP6) experimental design and organization. *Geosci. Model Dev.*, *9*(5), 1937-1958. https://doi.org/10.5194/gmd-9-1937-2016
Fahad, S., Bajwa, A. A., Nazir, U., Anjum, S. A., Farooq, A., Zohaib, A., . . . Huang, J. (2017). Crop Production under Drought and Heat Stress: Plant Responses and Management Options [Review]. *8*. https://doi.org/10.3389/fpls.2017.01147
Fischer, E. M., & Knutti, R. (2015). Anthropogenic contribution to global occurrence of heavy-precipitation and high-temperature extremes. *Nature Climate Change*, *5*(6), 560-564. https://doi.org/10.1038/nclimate2617
Florczyk, A., Melchiorri, M., Corbane, C., Schiavina, M., Maffenini, M., Pesaresi, M., . . . Ehrlich, D. (2019). Description of the GHS urban centre database 2015. *Public Release*.
Hausfather, Z., Marvel, K., Schmidt, G. A., Nielsen-Gammon, J. W., & Zelinka, M. (2022). Climate simulations: recognize the 'hot model'problem. In: Nature Publishing Group.
Heinicke, S., Frieler, K., Jägermeyr, J., & Mengel, M. (2022). Global gridded crop models underestimate yield responses to droughts and heatwaves. *Environmental Research Letters*, *17*(4), 044026. https://doi.org/10.1088/1748-9326/ac592e
Horton, R. M., Mankin, J. S., Lesk, C., Coffel, E., & Raymond, C. (2016). A review of recent advances in research on extreme heat events. *Current Climate Change Reports*, *2*(4), 242-259.
Hurtt, G. C., Chini, L., Sahajpal, R., Frolking, S., Bodirsky, B. L., Calvin, K., . . . Zhang, X. (2020). Harmonization of global land use change and management for the period 850–2100 (LUH2) for CMIP6. *Geosci. Model Dev.*, *13*(11), 5425-5464. https://doi.org/10.5194/gmd-13-5425-2020
Iizumi, T., Kim, W., & Nishimori, M. (2019). Modeling the Global Sowing and Harvesting Windows of Major Crops Around the Year 2000. *Journal of Advances in Modeling Earth Systems*, *11*(1), 99-112. https://doi.org/https://doi.org/10.1029/2018MS001477
India, G. o. (2018). Agricultural Statistics at a Glance 2012.
IPCC. (2022). *Summary for Policymakers. In: Climate Change 2022: Mitigation of Climate Change*.
Iso, B. (2017). 7243: Ergonomics of the thermal environment—assessment of heat stress using the wbgt (wet bulb globe temperature) index. *Int Org Standard*

Geneva Switzerland.
Ivanova, M., Baste, I., Lee, B., Belliethathan, S., Abdel Gelil, I., Gupta, J., . . . Mohamed-Katerere, J. C. (2012). Global Environmental Outlook 5, United Nations Environment Programme: Chapter 17, Global Responses.
Jacobson, A. P., Riggio, J., M. Tait, A., & E. M. Baillie, J. (2019). Global areas of low human impact ('Low Impact Areas') and fragmentation of the natural world. *Scientific Reports*, *9*(1), 14179. https://doi.org/10.1038/s41598-019-50558-6
Jägermeyr, J., Müller, C., Ruane, A. C., Elliott, J., Balkovic, J., Castillo, O., . . . Rosenzweig, C. (2021). Climate impacts on global agriculture emerge earlier in new generation of climate and crop models. *Nature Food*, *2*(11), 873-885. https://doi.org/10.1038/s43016-021-00400-y
Jonas Jägermeyr, C. M., Sara Minoli, Deepak Ray, & Stefan Siebert. (2021). *GGCMI Phase 3 crop calendar* https://doi.org/https://doi.org/10.5281/zenodo.5062513
Jones, B., & O'Neill, B. C. (2016). Spatially explicit global population scenarios consistent with the Shared Socioeconomic Pathways. *Environmental Research Letters*, *11*(8), 084003. https://doi.org/10.1088/1748-9326/11/8/084003
Jones, B., O'Neill, B. C., McDaniel, L., McGinnis, S., Mearns, L. O., & Tebaldi, C. (2015). Future population exposure to US heat extremes. *Nature Climate Change*, *5*(7), 652-655. https://doi.org/10.1038/nclimate2631
Kang, Y., Khan, S., & Ma, X. (2009). Climate change impacts on crop yield, crop water productivity and food security – A review. *Progress in Natural Science*, *19*(12), 1665-1674. https://doi.org/https://doi.org/10.1016/j.pnsc.2009.08.001
Kilasi, N. L., Singh, J., Vallejos, C. E., Ye, C., Jagadish, S. V. K., Kusolwa, P., & Rathinasabapathi, B. (2018). Heat Stress Tolerance in Rice (Oryza sativa L.): Identification of Quantitative Trait Loci and Candidate Genes for Seedling Growth Under Heat Stress [Original Research]. *9*. https://doi.org/10.3389/fpls.2018.01578
Klein Goldewijk, K., Beusen, A., Doelman, J., & Stehfest, E. (2017). Anthropogenic land use estimates for the Holocene–HYDE 3.2. *Earth System Science Data*, *9*(2), 927-953.
Laborte, A. G., Gutierrez, M. A., Balanza, J. G., Saito, K., Zwart, S. J., Boschetti, M., . . . Nelson, A. (2017). RiceAtlas, a spatial database of global rice calendars and production. *Scientific Data*, *4*(1), 170074. https://doi.org/10.1038/sdata.2017.74
Lambin, E. F., & Meyfroidt, P. (2011). Global land use change, economic globalization, and the looming land scarcity. *Proceedings of the National Academy of Sciences*, *108*(9), 3465-3472.
Lange, S. (2019). Trend-preserving bias adjustment and statistical downscaling with ISIMIP3BASD (v1.0). *Geoscientific Model Development*, *12*(7), 3055-3070. https://doi.org/10.5194/gmd-12-3055-2019
Lange, S. (2021). ISIMIP3BASD v2.5.0. https://doi.org/https://doi.org/10.5281/zenodo.4686991
Lange, S., Menz, C., Gleixner, S., Cucchi, M., Weedon, G. P., Amici, A., . . . Buontempo, C. (2021). WFDE5 over land merged with ERA5 over the ocean (W5E5 v2. 0).

Li, D., Yuan, J., & Kopp, R. E. (2020). Escalating global exposure to compound heat-humidity extremes with warming. *Environmental Research Letters*, *15*(6), 064003. https://doi.org/10.1088/1748-9326/ab7d04

Liljegren, J. C., Carhart, R. A., Lawday, P., Tschopp, S., & Sharp, R. (2008). Modeling the Wet Bulb Globe Temperature Using Standard Meteorological Measurements. *Journal of Occupational and Environmental Hygiene*, *5*(10), 645-655. https://doi.org/10.1080/15459620802310770

Luber, G., & McGeehin, M. (2008). Climate change and extreme heat events. *American journal of preventive medicine*, *35*(5), 429-435.

Luo, Y., Zhang, Z., Chen, Y., Li, Z., & Tao, F. (2020). ChinaCropPhen1km: a high-resolution crop phenological dataset for three staple crops in China during 2000–2015 based on leaf area index (LAI) products. *Earth Syst. Sci. Data*, *12*(1), 197-214. https://doi.org/10.5194/essd-12-197-2020

Mishra, V., Ganguly, A. R., Nijssen, B., & Lettenmaier, D. P. (2015). Changes in observed climate extremes in global urban areas. *Environmental Research Letters*, *10*(2), 024005. https://doi.org/10.1088/1748-9326/10/2/024005

Morse, N. B., Pellissier, P. A., Cianciola, E. N., Brereton, R. L., Sullivan, M. M., Shonka, N. K., . . . McDowell, W. H. (2014). Novel ecosystems in the Anthropocene

a revision of the novel ecosystem concept for pragmatic applications. *Ecology and society*, *19*(2). http://www.jstor.org/stable/26269579

Moss, R. H., Edmonds, J. A., Hibbard, K. A., Manning, M. R., Rose, S. K., van Vuuren, D. P., . . . Wilbanks, T. J. (2010). The next generation of scenarios for climate change research and assessment. *Nature*, *463*(7282), 747-756. https://doi.org/10.1038/nature08823

Mucina, L. (2019). Biome: evolution of a crucial ecological and biogeographical concept. *New Phytologist*, *222*(1), 97-114. https://doi.org/https://doi.org/10.1111/nph.15609

National Weather Service. (2022). *WetBulb Globe Temperature*. Retrieved May, 16th from https://www.weather.gov/tsa/wbgt

NOAA. (2014). *The Heat Index Equation*. Retrieved 19th May from https://www.wpc.ncep.noaa.gov/html/heatindex_equation.shtml

O'Neill, B. C., Tebaldi, C., van Vuuren, D. P., Eyring, V., Friedlingstein, P., Hurtt, G., . . . Sanderson, B. M. (2016). The Scenario Model Intercomparison Project (ScenarioMIP) for CMIP6. *Geosci. Model Dev.*, *9*(9), 3461-3482. https://doi.org/10.5194/gmd-9-3461-2016

Ogle, S. M., Domke, G., Kurz, W. A., Rocha, M. T., Huffman, T., Swan, A., . . . Krug, T. (2018). Delineating managed land for reporting national greenhouse gas emissions and removals to the United Nations framework convention on climate change. *Carbon balance and management*, *13*(1), 1-13.

Perkins, S. E. (2015). A review on the scientific understanding of heatwaves—Their measurement, driving mechanisms, and changes at the global scale. *Atmospheric Research*, *164*, 242-267.

Popp, A., Calvin, K., Fujimori, S., Havlik, P., Humpenöder, F., Stehfest, E., . . . Gusti, M. (2017). Land-use futures in the shared socio-economic pathways. *Global*

environmental change, *42*, 331-345.
Portmann, F. T., Siebert, S., & Döll, P. (2010). MIRCA2000—Global monthly irrigated and rainfed crop areas around the year 2000: A new high-resolution data set for agricultural and hydrological modeling. *Global Biogeochemical Cycles*, *24*(1). https://doi.org/https://doi.org/10.1029/2008GB003435
Poudel, P. B., Poudel, M. R. J. J. o. B., & World, T. s. (2020). Heat stress effects and tolerance in wheat: A review. *9*(3), 1-6.
Riahi, K., Van Vuuren, D. P., Kriegler, E., Edmonds, J., O'neill, B. C., Fujimori, S., . . . Fricko, O. (2017). The shared socioeconomic pathways and their energy, land use, and greenhouse gas emissions implications: an overview. *Global environmental change*, *42*, 153-168.
Ritchie, H. (2019). Who has contributed most to global CO2 emissions. *Our World in Data*, *1*.
Rockström, J., Steffen, W., Noone, K., Persson, Å., Chapin III, F. S., Lambin, E., . . . Schellnhuber, H. J. (2009). Planetary boundaries: exploring the safe operating space for humanity. *Ecology and society*, *14*(2).
Rogelj, J., den Elzen, M., Hohne, N., Fransen, T., Fekete, H., Winkler, H., . . . Meinshausen, M. (2016). Paris Agreement climate proposals need a boost to keep warming well below 2 degrees C. *Nature*, *534*(7609), 631-639. https://doi.org/10.1038/nature18307
Sabagh, A. E., Hossain, A., Iqbal, M. A., Barutçular, C., Islam, M. S., Çiğ, F., . . . Wasaya, A. (2020a). Maize adaptability to heat stress under changing climate. In *Plant stress physiology*. IntechOpen.
Sabagh, A. E., Hossain, A., Islam, M. S., Iqbal, M. A., Fahad, S., Ratnasekera, D., & Llanes, A. (2020b). Consequences and mitigation strategies of heat stress for sustainability of soybean (Glycine max L. Merr.) production under the changing climate. *Plant stress physiology*.
Sachs, J., Kroll, C., Lafortune, G., Fuller, G., & Woelm, F. (2021). *Sustainable development report 2021*. Cambridge University Press.
Sacks, W. J., Deryng, D., Foley, J. A., & Ramankutty, N. (2010). Crop planting dates: an analysis of global patterns. *Global Ecology and Biogeography*, *19*(5), 607-620. https://doi.org/https://doi.org/10.1111/j.1466-8238.2010.00551.x
Sanderson, E. W., Walston, J., & Robinson, J. G. (2018). From Bottleneck to Breakthrough: Urbanization and the Future of Biodiversity Conservation. *Bioscience*, *68*(6), 412-426. https://doi.org/10.1093/biosci/biy039
Stefan Lange, M. B. (2021). *ISIMIP3b bias-adjusted atmospheric climate input data (v1.1). ISIMIP Repository.* https://doi.org/https://doi.org/10.48364/ISIMIP.842396.1
Sulikowska, A., & Wypych, A. (2020). Summer temperature extremes in Europe: how does the definition affect the results? *Theoretical and Applied Climatology*, *141*(1), 19-30. https://doi.org/10.1007/s00704-020-03166-8
Tiwari, Y. K., & Yadav, S. K. (2019). High Temperature Stress Tolerance in Maize (Zea mays L.): Physiological and Molecular Mechanisms. *Journal of Plant Biology*, *62*(2), 93-102. https://doi.org/10.1007/s12374-018-0350-x

Tuholske, C., Caylor, K., Funk, C., Verdin, A., Sweeney, S., Grace, K., . . . Evans, T. (2021). Global urban population exposure to extreme heat. *Proc Natl Acad Sci U S A*, *118*(41). https://doi.org/10.1073/pnas.2024792118

UNCCD. (2017). Global land outlook.

van der Wielen, W. (2021). *Exploring the Anthropocene: Mapping land-system change until 2100 under the Shared Socio-economic Pathways*
Utrecht University].

van Vuuren, D. P., Edmonds, J., Kainuma, M., Riahi, K., Thomson, A., Hibbard, K., . . . Rose, S. K. (2011). The representative concentration pathways: an overview. *Climatic Change*, *109*(1), 5. https://doi.org/10.1007/s10584-011-0148-z

van Vuuren, D. P., Kriegler, E., O'Neill, B. C., Ebi, K. L., Riahi, K., Carter, T. R., . . . Winkler, H. (2014). A new scenario framework for Climate Change Research: scenario matrix architecture. *Climatic Change*, *122*(3), 373-386. https://doi.org/10.1007/s10584-013-0906-1

Verburg, P. H., Crossman, N., Ellis, E. C., Heinimann, A., Hostert, P., Mertz, O., . . . Golubiewski, N. (2015). Land system science and sustainable development of the earth system: A global land project perspective. *Anthropocene*, *12*, 29-41.

Verburg, P. H., Erb, K.-H., Mertz, O., & Espindola, G. (2013). Land System Science: between global challenges and local realities. *Current Opinion in Environmental Sustainability*, *5*(5), 433-437. https://doi.org/https://doi.org/10.1016/j.cosust.2013.08.001

Vuuren, D. v. (2022). *UU, me and the IPCC*.

Wahid, A., Gelani, S., Ashraf, M., & Foolad, M. (2007). Heat tolerance in plants: An overview. *Environmental and Experimental Botany*, *61*(3), 199-223. https://doi.org/10.1016/j.envexpbot.2007.05.011

Warszawski, L., Frieler, K., Huber, V., Piontek, F., Serdeczny, O., & Schewe, J. (2014). The inter-sectoral impact model intercomparison project (ISI–MIP): project framework. *Proceedings of the National Academy of Sciences*, *111*(9), 3228-3232.

Whitcraft, A. K., Becker-Reshef, I., & Justice, C. O. (2015). Agricultural growing season calendars derived from MODIS surface reflectance. *International Journal of Digital Earth*, *8*(3), 173-197. https://doi.org/10.1080/17538947.2014.894147

7. Appendix

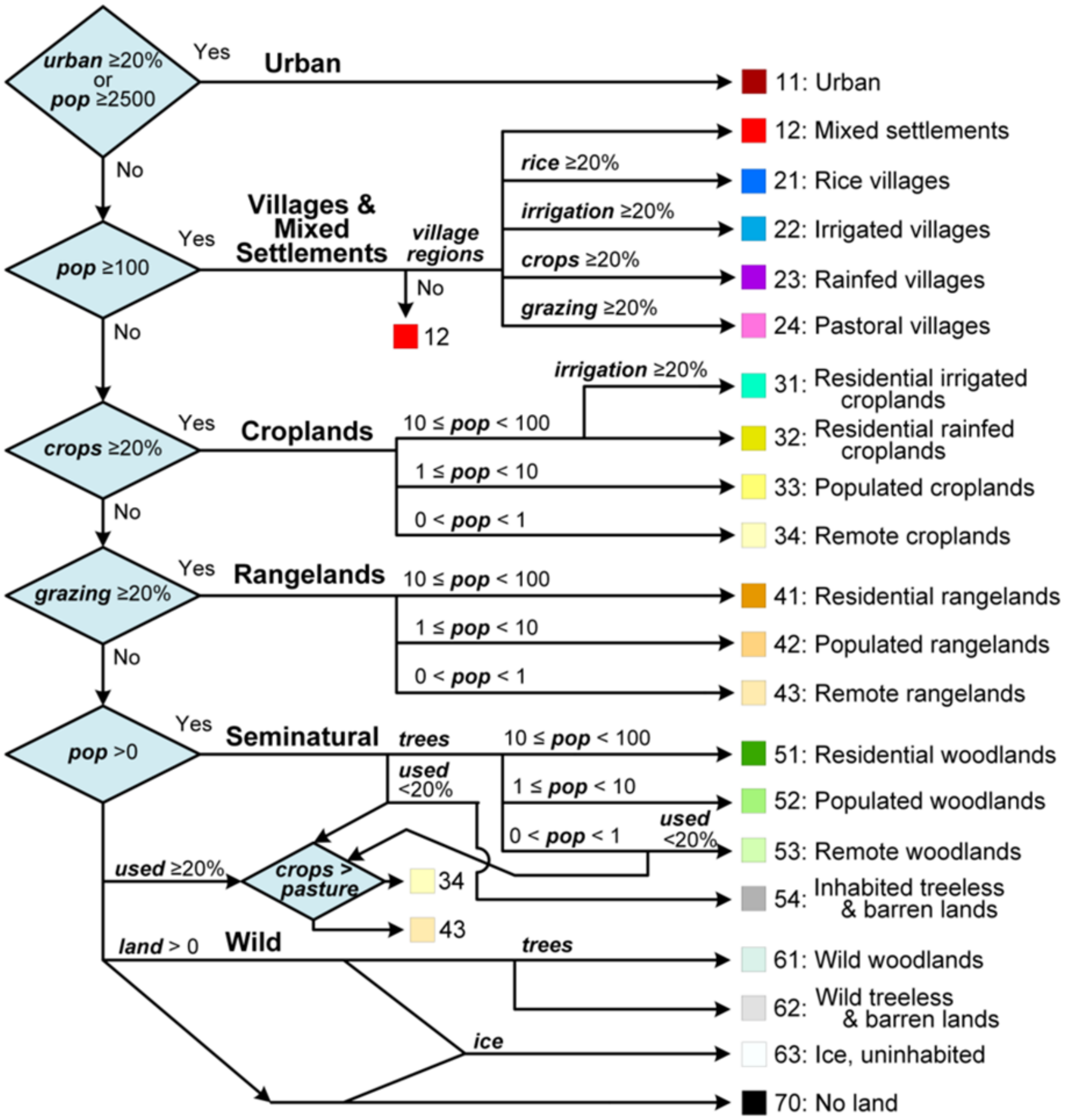

Figure A-1: anthrome classification method, retirved from (van der Wielen, 2021)

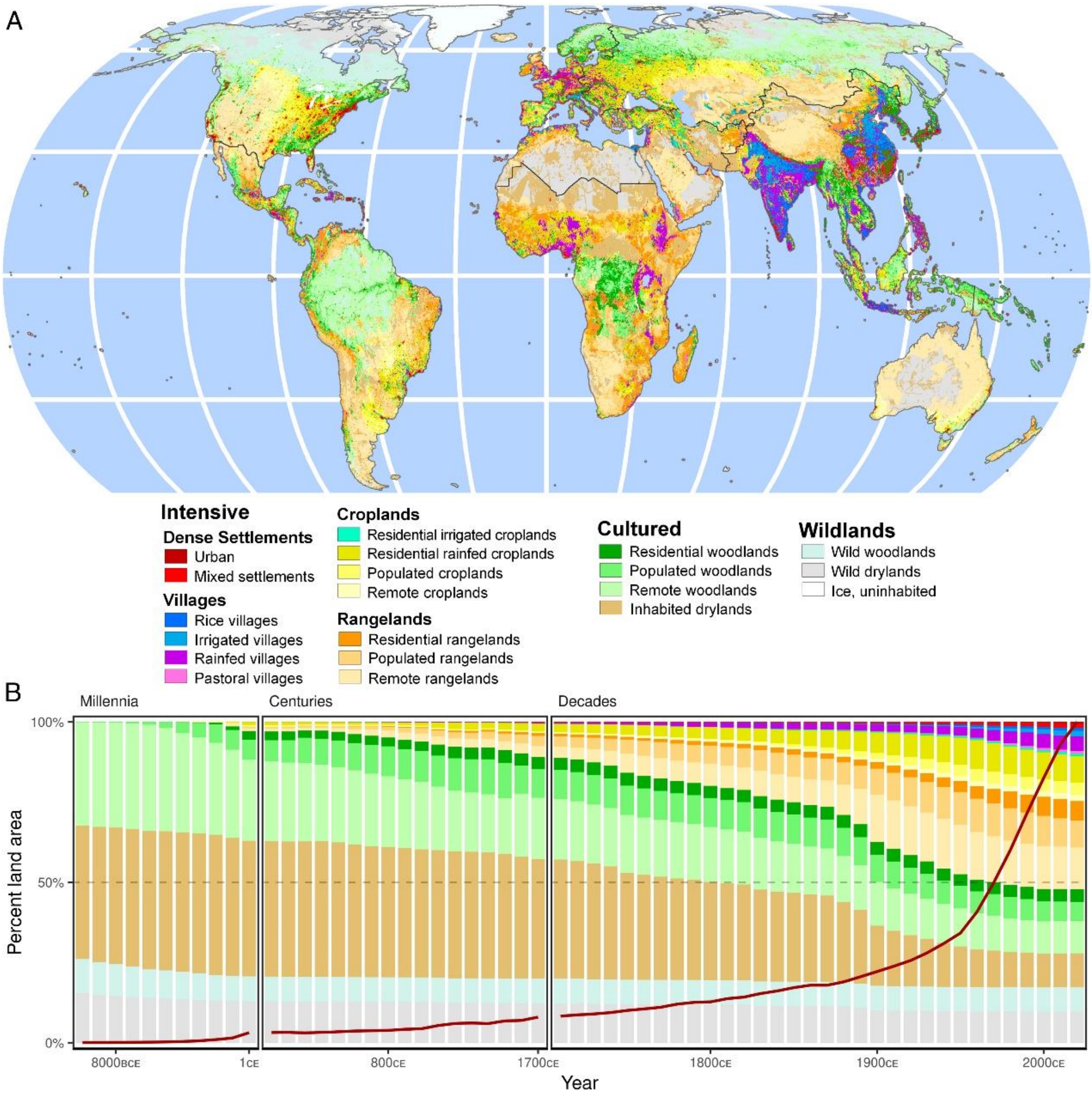

Figure A-2: anthrome classification, retrieved from (Ellis et al., 2021)

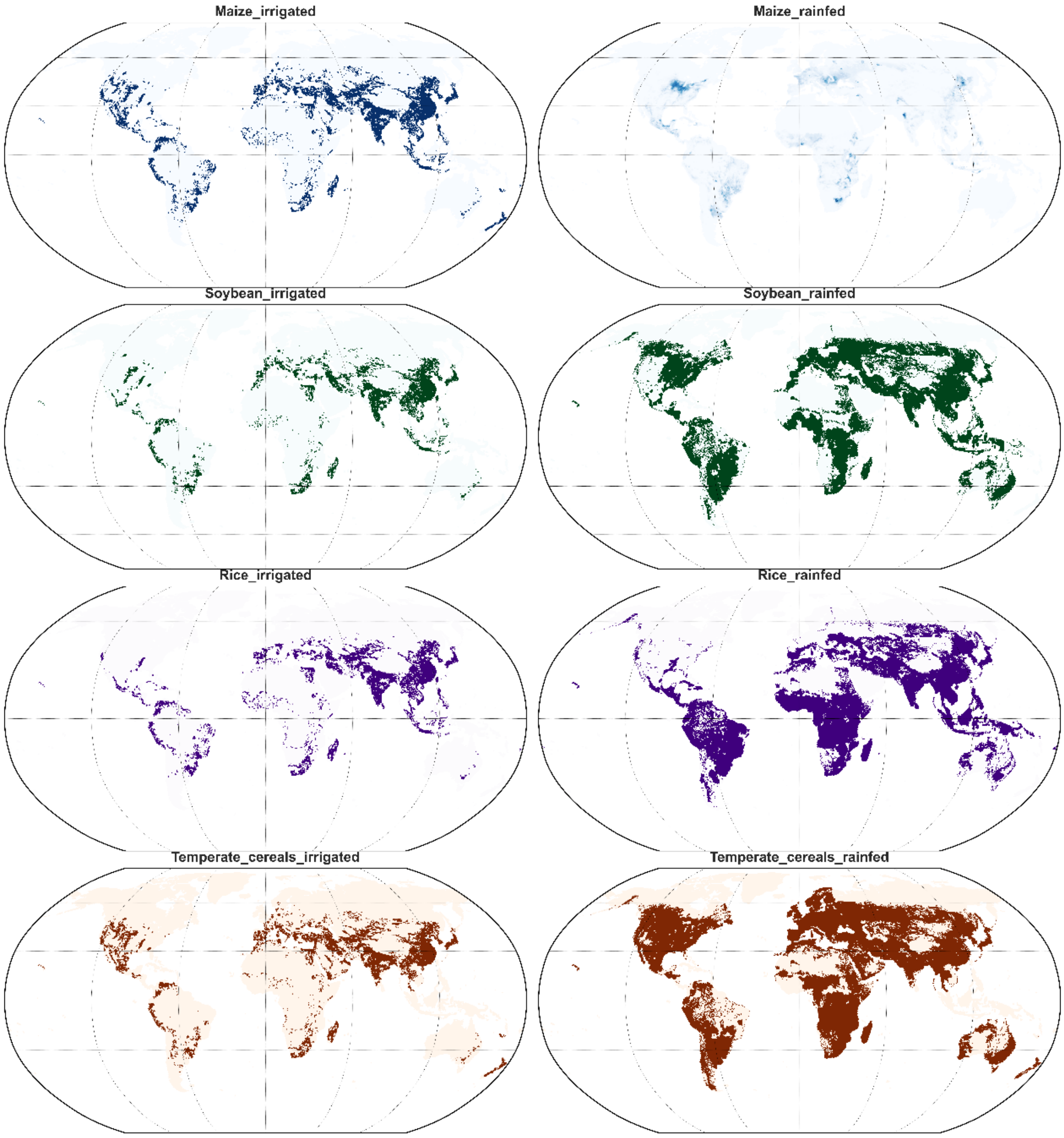

Figure A-3: harvested area of four crops(Maize, Soybean, Rice, Wheat)

Table A-1: frequency of extreme heat days in 2015 and 2100 for three scenarios

Scenarios	ssp126		ssp370		ssp585	
Year / Name	2015	2100	2015	2100	2015	2100
Urban	48	90	45	209	47	219
Mixed settlements	47	114	42	227	47	238
Rice villages	37	76	39	186	41	200
Irrigated villages	45	75	42	176	41	200
Rainfed villages	50	136	41	275	50	281
Pastoral villages	48	143	44	264	48	285
Residential irrigated croplands	46	70	43	150	43	181
Residential rainfed croplands	50	105	46	216	50	253
Populated croplands	48	94	49	197	48	233
Remote croplands	55	104	54	200	49	264
Residential rangelands	53	128	48	243	53	275
Populated rangelands	48	96	47	181	49	225
Remote rangelands	61	93	57	188	53	213
Residential woodlands	52	108	39	231	49	247
Populated woodlands	46	113	45	226	47	254
Remote woodlands	47	108	48	213	48	252
Inhabited treeless & barren lands	52	107	49	195	50	227
Wild woodlands	48	88	47	188	48	219
Wild treeless & barren lands	55	80	50	150	49	173
Ice & uninhabited	47	52	48	90	47	97

Table A-2: population exposure to extreme heat events in 2015 and 2100 for three future scenarios

WBGT = 25°C						
Scenarios	ssp126		ssp370		ssp585	
Year / Name	2015	2100	2015	2100	2015	2100
Urban	5.32E+08	1.2E+09	5.23E+08	2.81E+09	5.62E+08	2.23E+09
Mixed settlements	4.16E+08	3.39E+08	4.23E+08	1.03E+09	4.22E+08	5.68E+08
Rice villages	4.55E+08	3.21E+08	4.56E+08	1.17E+09	4.54E+08	7.4E+08
Irrigated villages	18153512	36990344	16735650	1.25E+08	22019580	94955328
Rainfed villages	5.34E+08	6.18E+08	5.35E+08	1.5E+09	5.39E+08	7.13E+08
Pastoral villages	2.62E+08	4.2E+08	2.64E+08	1.08E+09	2.67E+08	5.28E+08
WBGT = 26°C						
Scenarios	ssp126		ssp370		ssp585	
Year / Name	2015	2100	2015	2100	2015	2100
Urban	5.23E+08	1.13E+09	5.1E+08	2.56E+09	5.21E+08	2.07E+09
Mixed settlements	3.93E+08	3.15E+08	3.59E+08	9.4E+08	3.98E+08	5.36E+08
Rice villages	4.47E+08	2.89E+08	4.46E+08	8.74E+08	4.46E+08	6.88E+08
Irrigated	149139	319847	145307	1.12E+0	161616	8201156

villages	04	96	43	8	95	8
Rainfed villages	5.08E+08	6.05E+08	4.53E+08	1.43E+09	5.21E+08	6.92E+08
Pastoral villages	2.54E+08	4.04E+08	2.5E+08	1.04E+09	2.55E+08	5.09E+08
WBGT = 28°C						
Scenarios	ssp126		ssp370		ssp585	
Year / Name	2015	2100	2015	2100	2015	2100
Urban	4.48E+08	9.84E+08	4.1E+08	2.24E+09	4.6E+08	1.58E+09
Mixed settlements	2.69E+08	2.44E+08	2.28E+08	8.05E+08	2.53E+08	4.43E+08
Rice villages	4.31E+08	2.63E+08	4.32E+08	6.33E+08	4.31E+08	4.91E+08
Irrigated villages	9445491	22133846	5670306	88653704	5920955	51916360
Rainfed villages	3.42E+08	5.22E+08	2.18E+08	1.39E+09	3.53E+08	6.47E+08
Pastoral villages	1.88E+08	3.36E+08	1.65E+08	9.98E+08	1.84E+08	4.63E+08
WBGT = 30°C						
Scenarios	ssp126		ssp370		ssp585	
Year / Name	2015	2100	2015	2100	2015	2100
Urban	2.77E+08	4.62E+08	2.8E+08	2.08E+09	3.03E+08	1.24E+09
Mixed settlements	1.79E+08	1.11E+08	1.83E+08	7.33E+08	1.8E+08	3.57E+08

Rice villages	4.17E+08	2.47E+08	4.2E+08	5.48E+08	4.15E+08	3.18E+08
Irrigated villages	4373759	4668655	4136213	80019888	4521844	39411316
Rainfed villages	1.44E+08	1.18E+08	1.47E+08	1.37E+09	1.45E+08	6.16E+08
Pastoral villages	1.23E+08	1.08E+08	1.26E+08	9.66E+08	1.24E+08	4.39E+08
WBGT = 33°C						
Scenarios	ssp126		ssp370		ssp585	
Year / Name	2015	2100	2015	2100	2015	2100
Urban	2.64E+08	2.88E+08	2.55E+08	1.58E+09	2.71E+08	1E+09
Mixed settlements	1.66E+08	83480616	1.67E+08	4.67E+08	1.64E+08	2.72E+08
Rice villages	4E+08	2.35E+08	3.97E+08	4.67E+08	3.97E+08	2.63E+08
Irrigated villages	3767319	3026482	3580115	23426076	3696824	20455280
Rainfed villages	1.35E+08	55322252	1.34E+08	1.06E+09	1.34E+08	5.67E+08
Pastoral villages	1.1E+08	65622660	1.06E+08	5.71E+08	1.07E+08	3.67E+08

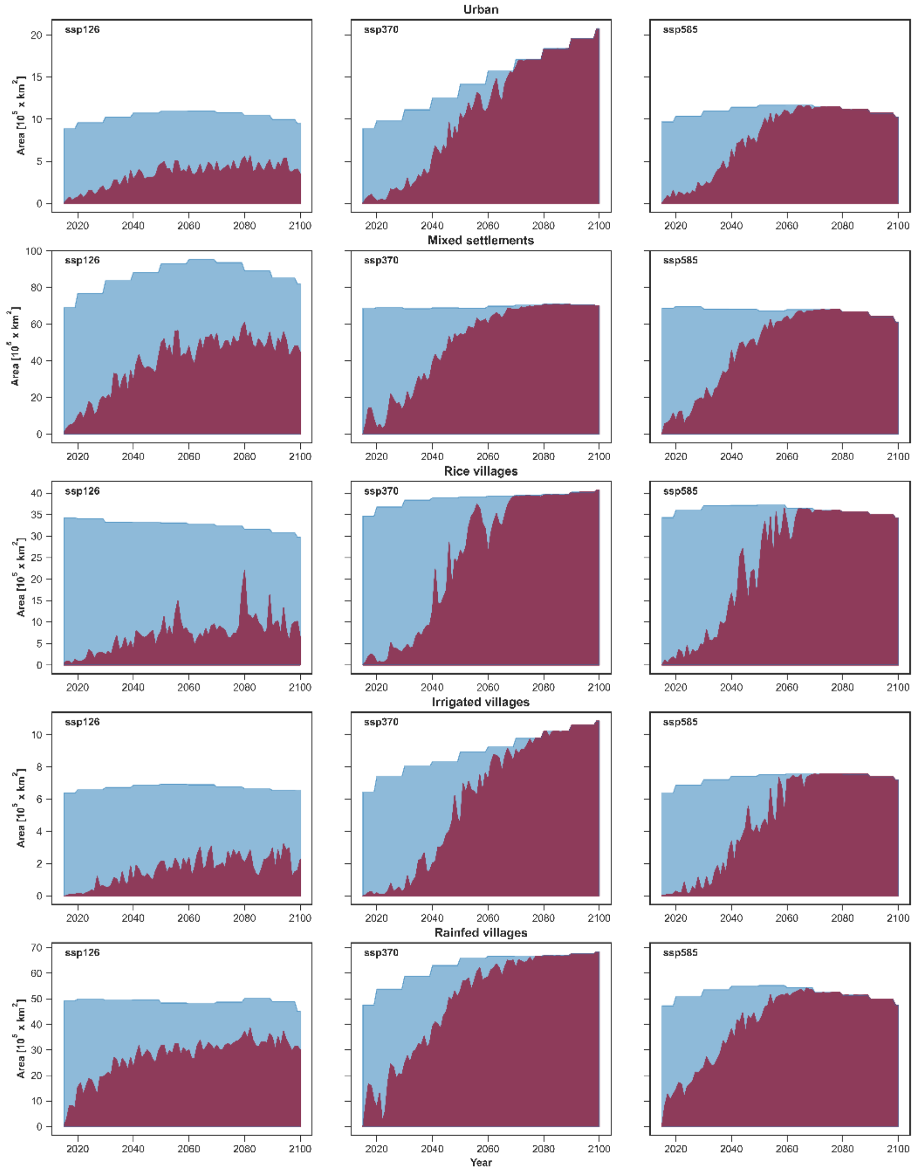

Figure A-4: area of each anthrome that experience extreme heat event(> 0day) (red part), bule part refers to total area of each anthrome (change every 10 years in IMAGE framwork)

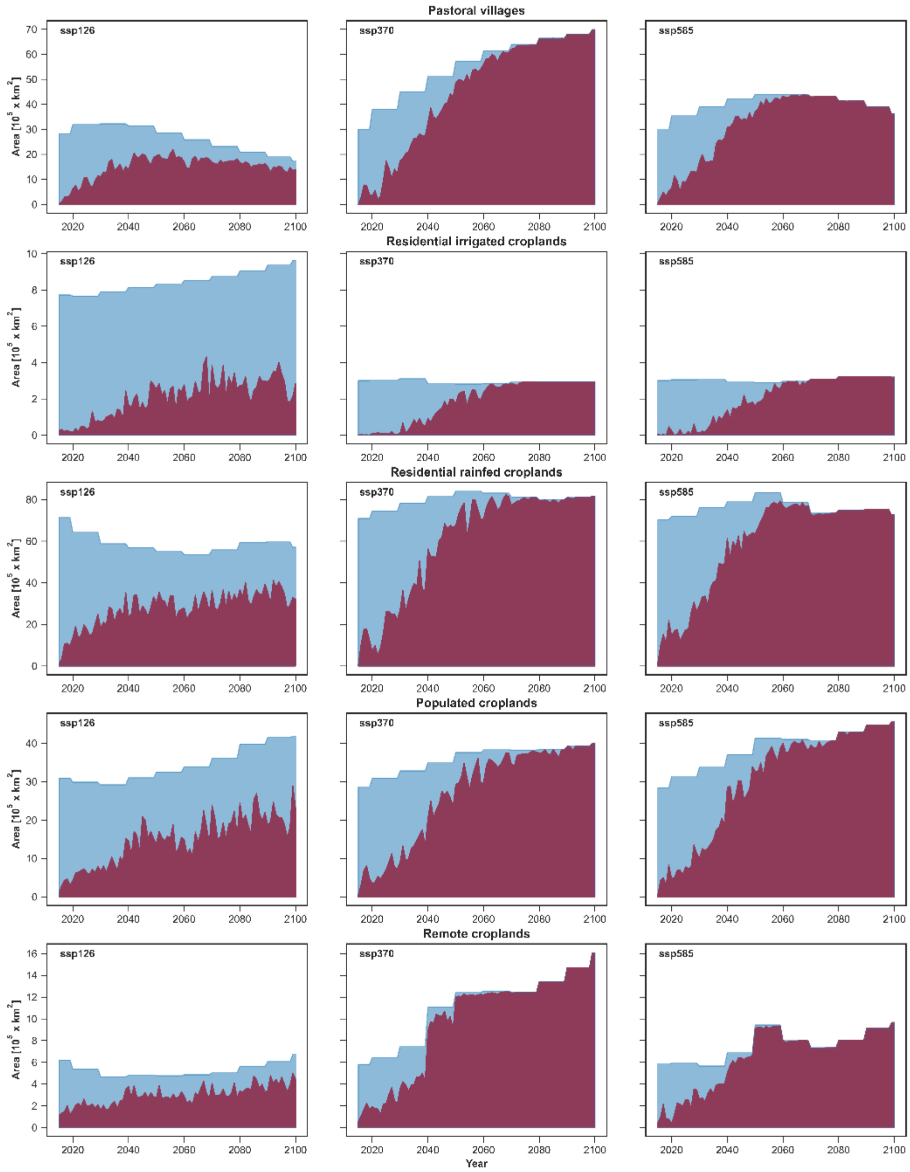

Figure A-5: area of each anthrome that experience extreme heat event(> 0 day) (red part), bule part refers to total area of each anthrome (change every 10 years in IMAGE framwork).

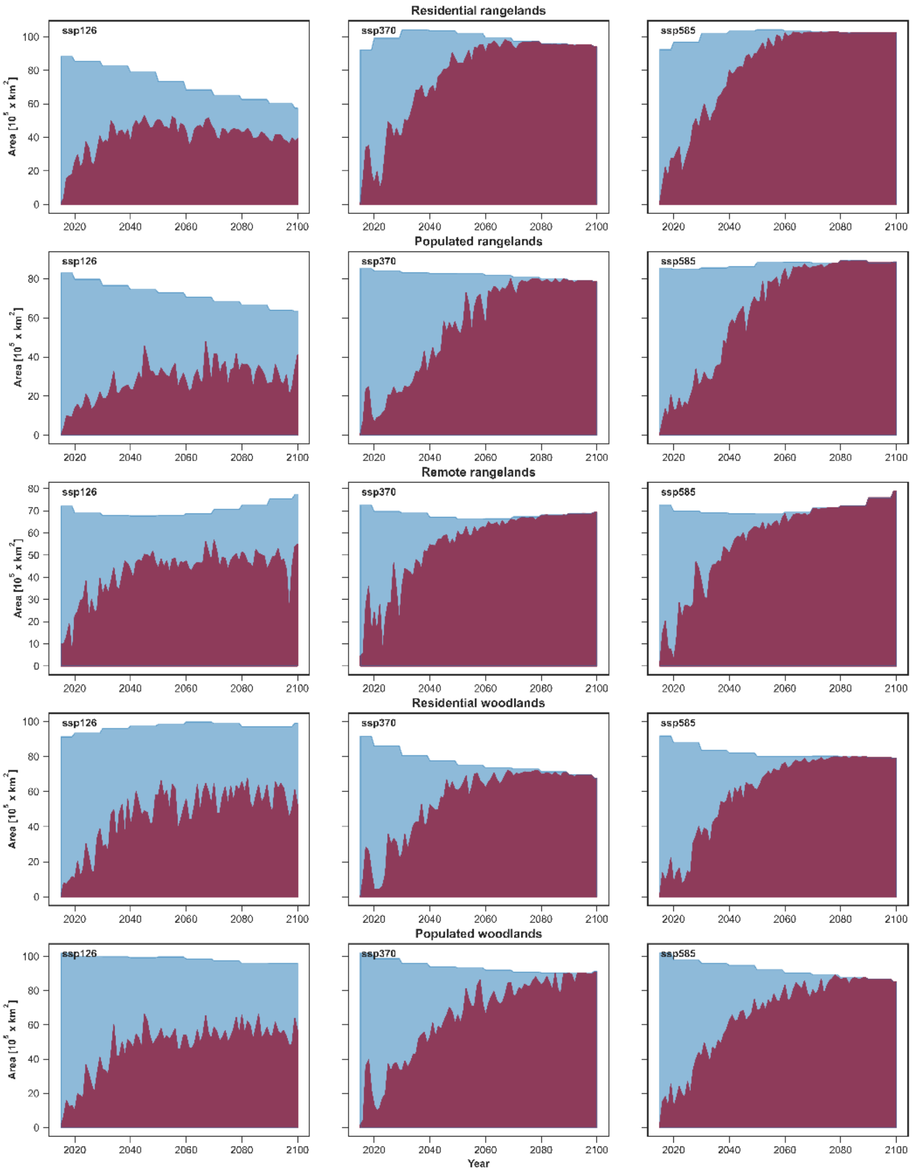

Figure A-6: area of each anthrome that experience extreme heat event(> 0 day) (red part), bule part refers to total area of each anthrome (change every 10 years in IMAGE framwork)

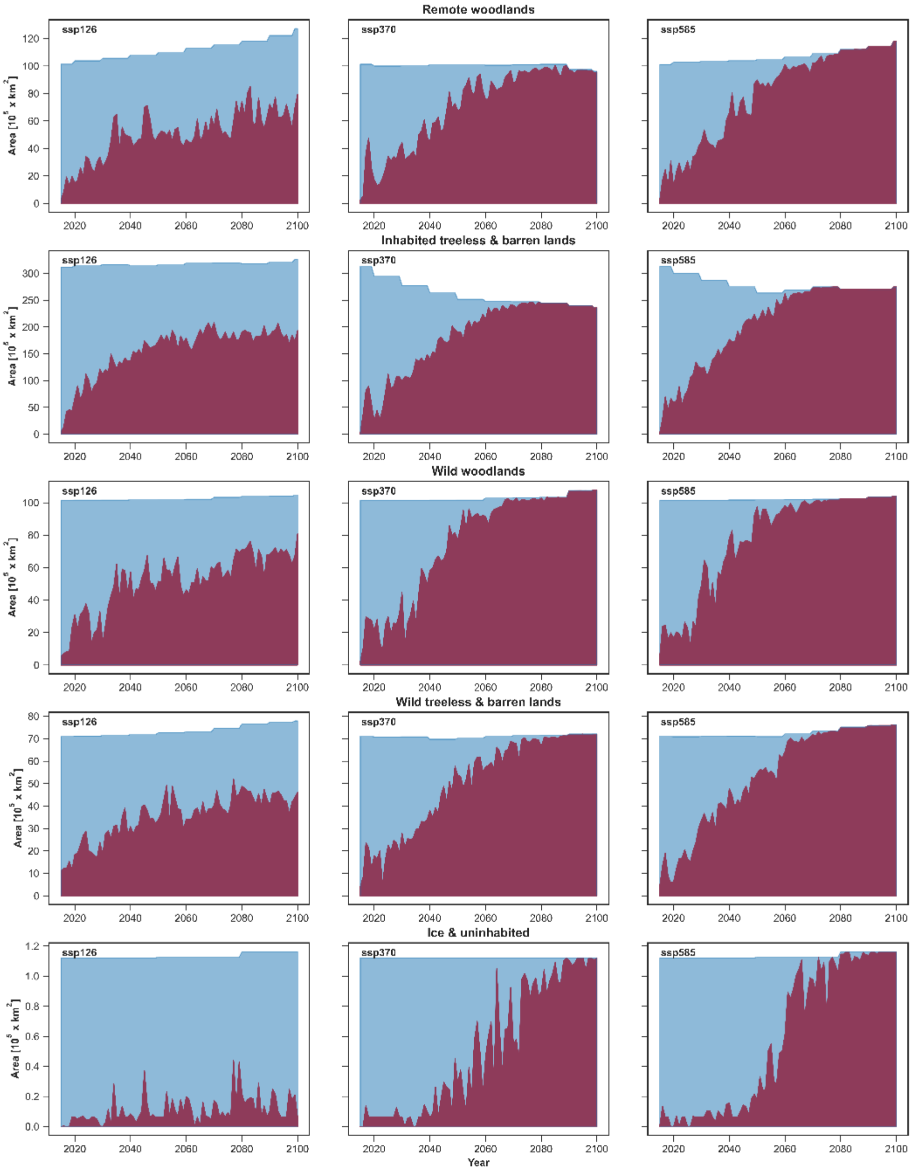

Figure A-7: area of each anthrome that experience extreme heat event(> 0 day) (red part), bule part refers to total area of each anthrome (change every 10 years in IMAGE framwork).

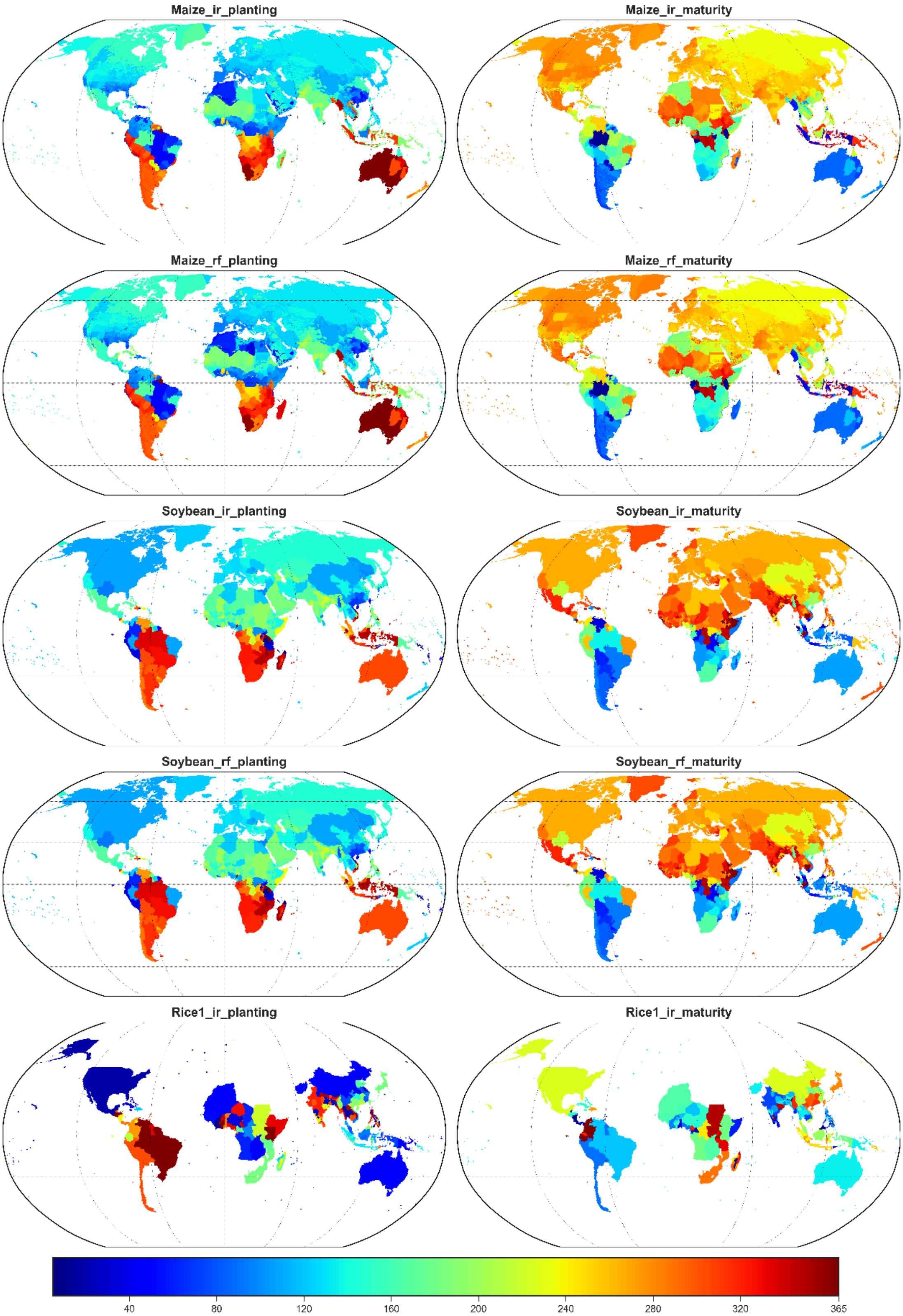

Figure A-8: GGCMI crop calendar of four major crops

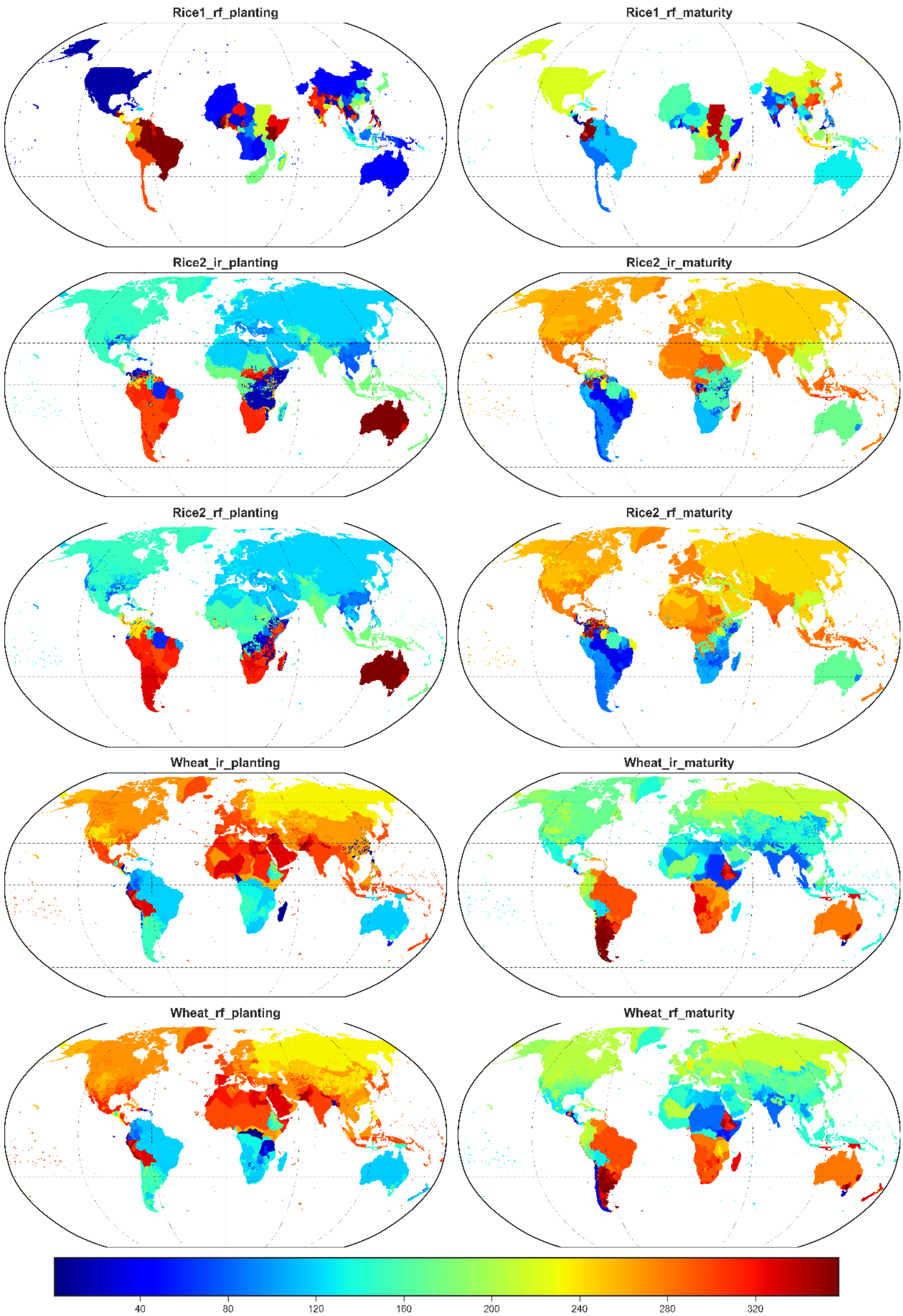

Figure A-9: GGCMI crop calendar of four major crops

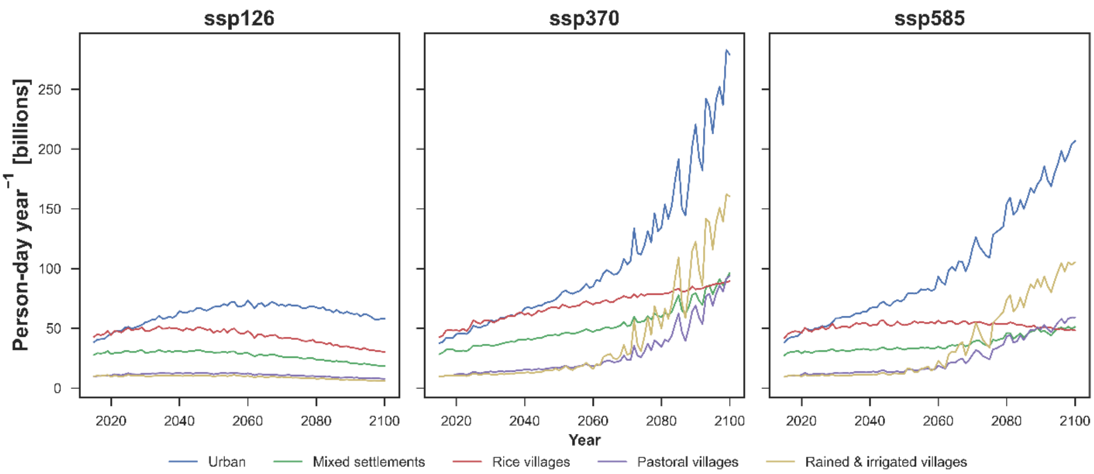

Figure A-10: population exposed to extreme heat in six high density anthrome from 2015 to 2100 (WBGT = 30°C), mean values of five GCMs.

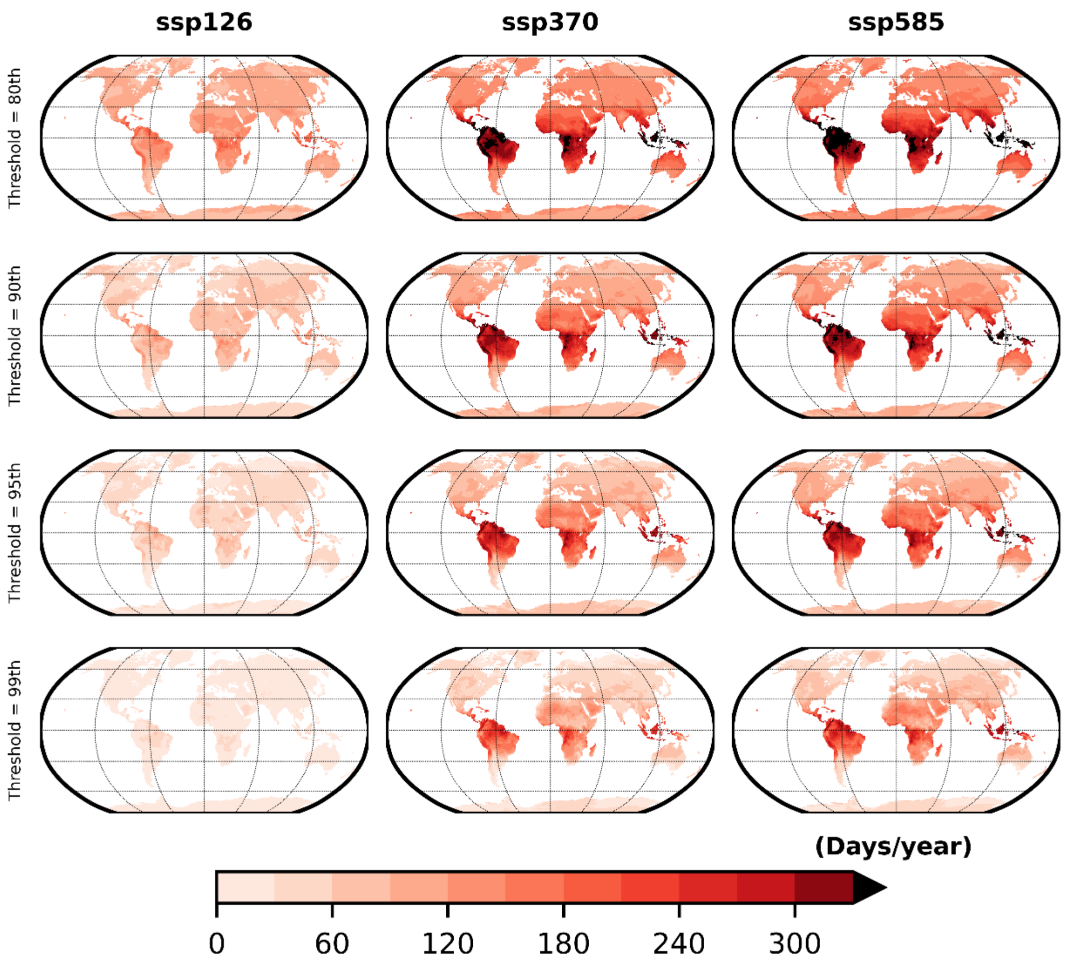

Figure A-11: extreme heat days of different temperature thresholds for three future scenarios

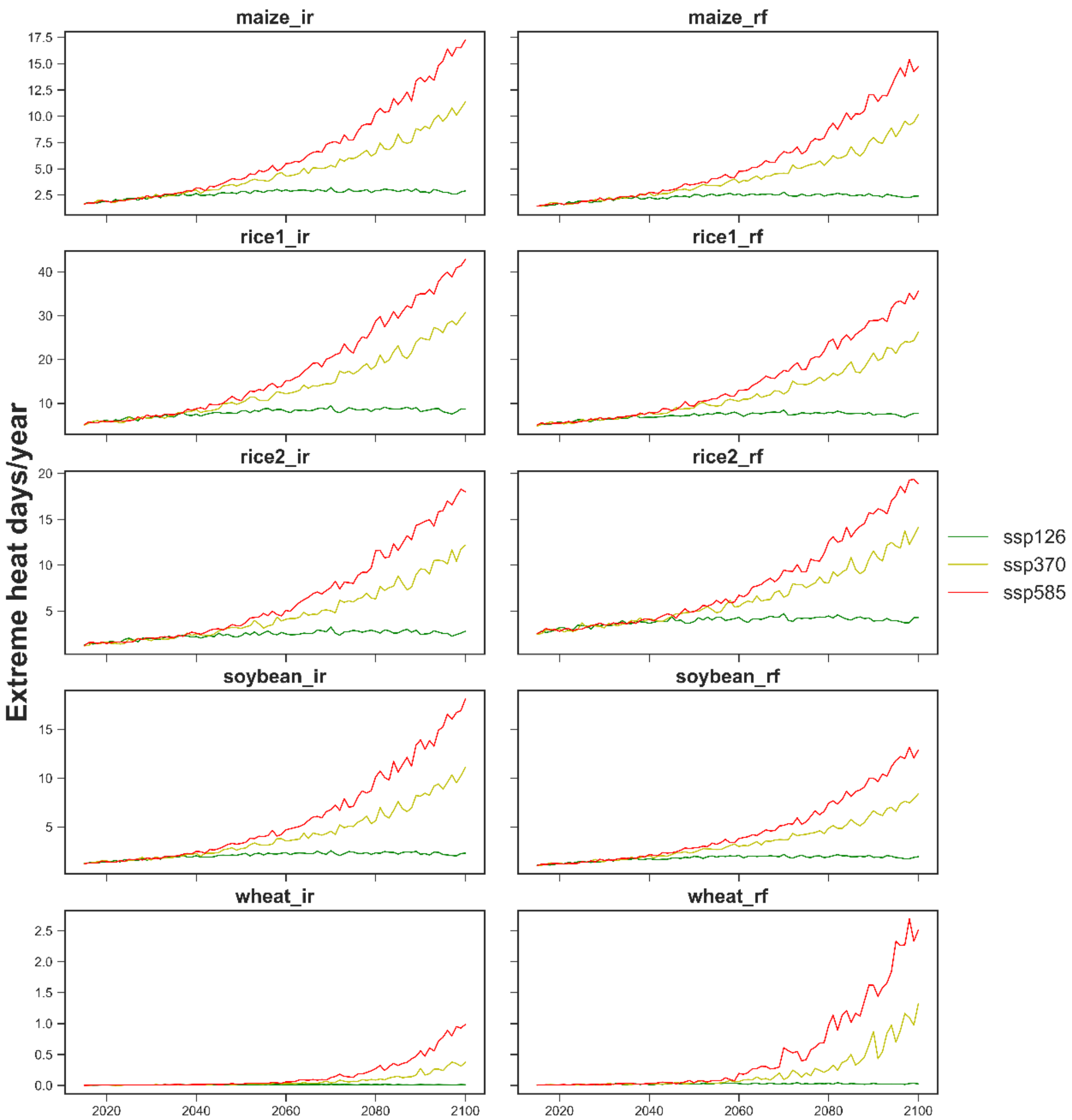

Figure A- 12: extreme heat days of crops for 3 future scenarios